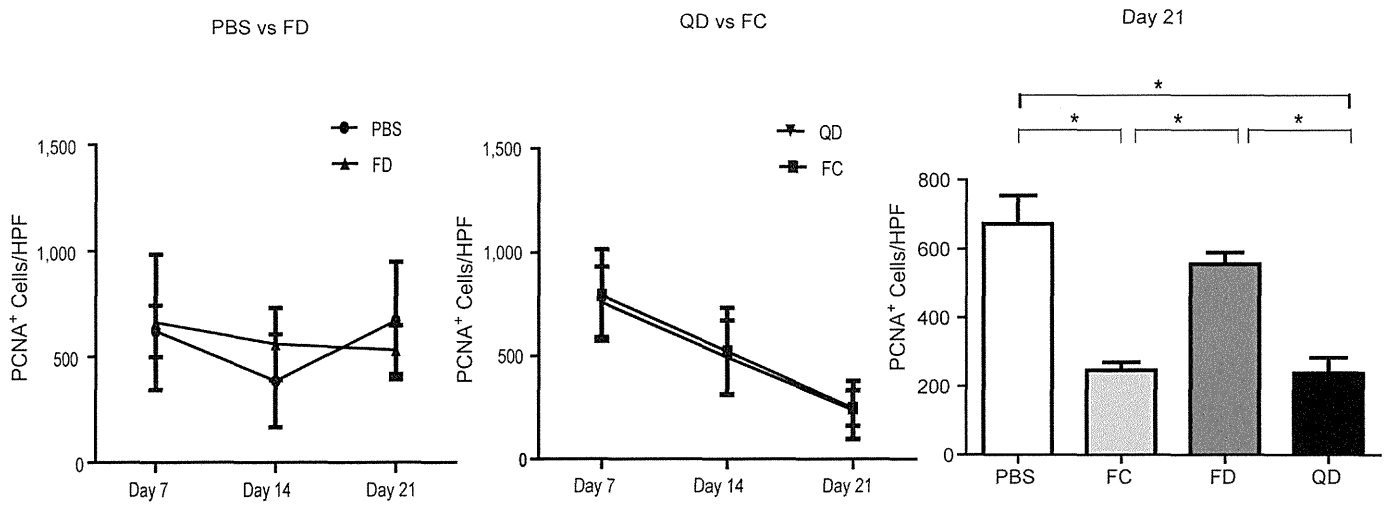

FIG. 7. Post-QQc diabetic progenitor cell therapy increases cellular proliferation in the wound. The *left* and *middle graphs* show the number of PCNA-positive cells in the wound per HPF on day 7, day 14, and day 21 in the following treated groups: PBS vs. freshly isolated diabetic cells (FD; *left*), QD vs. FC (*middle*). The *right bar graph* shows the number of PCNA-positive cells in the wound per HPF on day 21. *$P < 0.05$.

Kwon et al. (6) QQc is a serum-free culture system recently developed and reported by our group (27). QQc is a functional culture system that not only increases the number of EPCs but also increases the population of differentiated colony-forming EPCs (i.e., vasculogenic EPCs). Our in vitro experiments demonstrate that QQc significantly increases diabetic EPC cell number, definitive colony formation, and tubulization. Because QQc not only increased the number of diabetic EPCs but also restored their function to the level of control EPCs, we tested the effects of QQc diabetic EPCs ex vivo–expanded cells on wound closure. We used a stented wound closure model to minimize the effects of wound contracture (35). To focus our investigation on the function and efficacy of post-QQc diabetic EPCs compared with fresh healthy allogeneic EPCs, we selected a euglycemic wound closure mice model. We hypothesized that the use of a euglycemic recipient would eliminate the effect of confounding variables present in a diabetic recipient model.

Because new blood vessel formation is crucial for successful wound healing, we hypothesize that DM_{QQc} therapy leads to accelerated wound closure by enhancing vasculogenesis (36). CD31 staining demonstrated that post-QQc diabetic EPC treatment increased wound vascularity compared with freshly isolated diabetic EPC treatment and control groups at all time points. Moreover, as demonstrated previously by Masuda et al. (27,29), because QQc increases the number of dEPC-CFUs (i.e., vasculogenic EPCs) and dEPCs more readily form new vessels (compared with pEPCs), we hypothesize that they are the vitally important EPC fraction mediating the therapeutic vasculogenesis observed in our in vivo experiments. Collectively, our findings suggest a potential mechanism by which DM_{QQc} EPCs accelerate wound closure; transplanted post-QQc EPCs accelerate wound closure by forming tubules and inosculating with existing vasculature. This idea is further supported by the finding that GFP-labeled KSL cells incorporated into the native vascular network.

Enhanced new blood vessel formation may accelerate wound closure in a number of different ways. We found that DM_{QQc} therapy significantly enhanced the percentage of mature collagen in the wound. Interestingly, post-QQc diabetic EPCs exhibit significantly higher CD29mRNA expression compared with fresh diabetic EPCs. Recently, it was reported that CD29 directly influences growth factor signaling and promotes fibroblast migration (37). Together with the PCNA data, we hypothesize that DM_{QQc} stimulates fibroblast migration to the wound and accelerates wound closure.

To confirm the efficacy of QQc therapy in diabetic mice, we injected pre-QQc and post-QQc control and diabetic KSL cells to a full-thickness wound in STZ-induced glycemic diabetic mice. The results indicated that accelerated wound healing was seen only in post-QQc control KSL cell–treated group. The pre-diabetic and post-diabetic QQc KSL cells group, pre-QQc control KSL cells group, and the PBS-treated group demonstrated the same percent wound closure at all times from day 3 to day 21. In other words, the healing of post-QQc diabetic KSL cells in eugylcemic wounds was not seen in a diabetic condition. We assume from this result that hyperglycemic conditions of diabetic mice may have deteriorated the function of post-QQc diabetic KSL cells. Because post-QQc diabetic KSL cells have a highly therapeutic effect in euglycemic conditions, we believe that QQc therapy may be effective in euglycemic diabetic patients, i.e., patients with controlled blood glucose levels (blood glucose <8 mmol/L or <140 mg/dL) according to the practical guidelines on the management and prevention of diabetic foot (38). Our data are similar, and we daily treat diabetic patients with chronic wounds and high blood glucose. Many previous reports have shown that one of the standards of care for diabetic wounds involves systemic glucose control, and effective wound healing cannot be expected for uncontrolled diabetes even with highly effective therapy. Our results for EPC therapy for uncontrolled diabetic mice show that the condition of the host has a great impact on deterioration of the cells being administered, and we believe that "metabolic memory" and epigenetic modification by hyperglycemia are possibilities for why this is. In euglycemic diabetic patients the efficacy of EPC therapy for wound healing is limited because of autologous EPC vasculogenic dysfunction, as shown in our previous report (24). We believe that present EPC therapy with application of autologous dysfunctional EPC may not be effective even for diabetic patients with controlled glucose. The application of QQc in these patients may be the key for highly therapeutic autologous

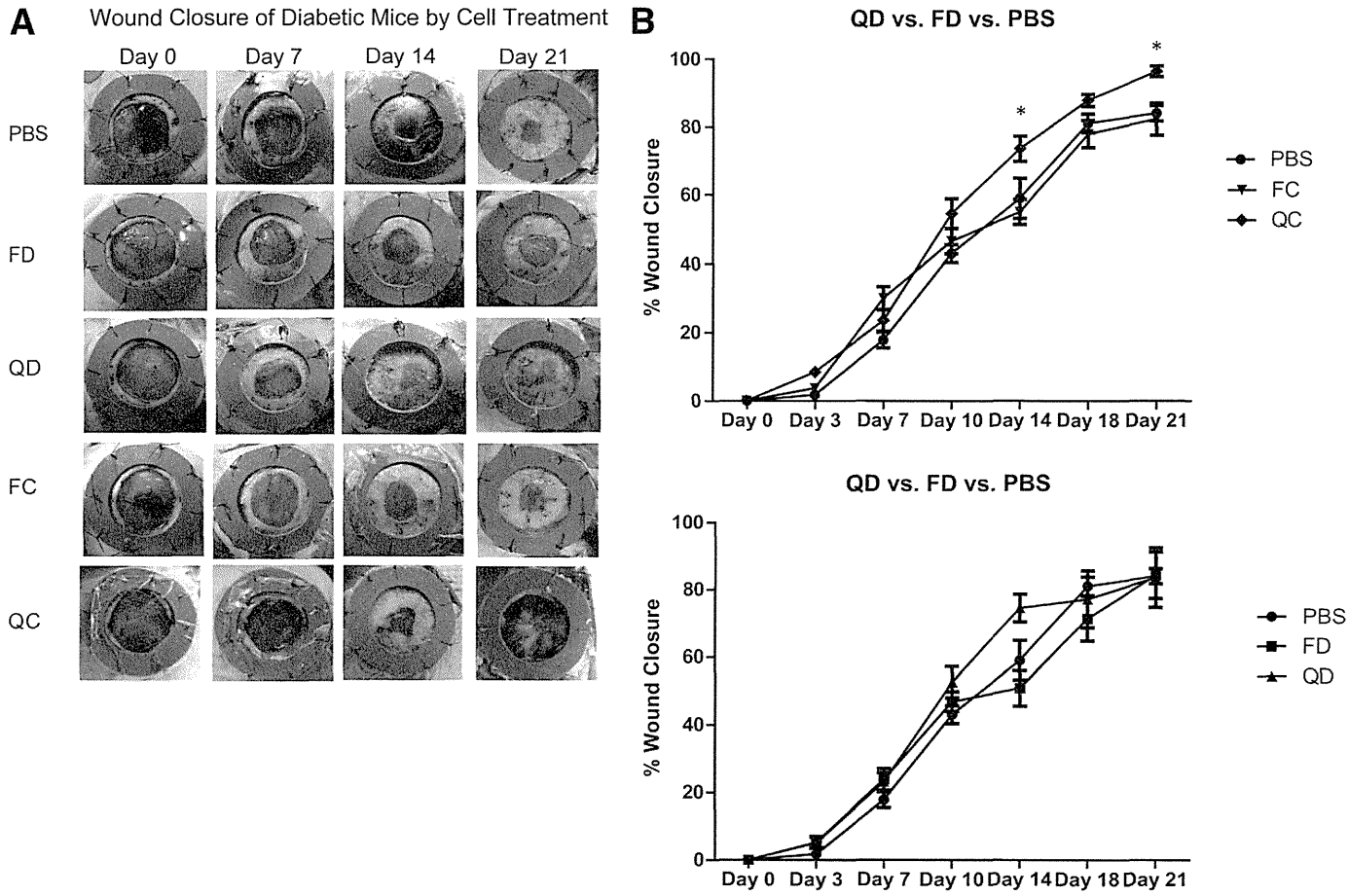

FIG. 8. Efficacy of post-QQc diabetic progenitor cell therapy is deteriorated by diabetic condition. *A*: Representative images show wound healing in STZ-induced diabetic mice treated with PBS, before and after control, and treated with diabetic QQc cells. Wounds were photographed at the times indicated, from day 0 to day 21. *B*: The graph shows the comparison of percent wound closure between post-QQc control cell (QC)-treated vs. freshly isolated control cell (FC)-treated vs. PBS-treated groups. QC indicated significant percent wound closure compared with FC and PBS on day 14 (QC: 73.60 ± 3.69 vs. FC: 55.02 ± 3.61 vs. PBS: 58.98 ± 5.86%; $P < 0.05$) and day 21 (QC: 96.34 ± 1.52 vs. FC: 82.29 ± 4.72 vs. PBS: 84.01 ± 2.28%; $P < 0.05$). The wound closure between FC and PBS was similar without any significance. *C*: The graph shows the comparison of percent wound closure between QD-treated vs. freshly isolated diabetic cell (FD)-treated vs. PBS-treated groups. There was no significant difference between the three compared groups at all time points. *$P < 0.05$.

diabetic EPC therapy. To test our hypothesis, we have tried to establish a stented wound healing model of insulin-treated STZ diabetic mice with controlled glucose levels and treated these mice with diabetic pre-QQc and post-QQc KSL cells. Unfortunately, the model was difficult to establish because of the many interventions on the mice. Therefore, this hypothesis remains to be proven.

Another limitation of our study includes not knowing the exact mechanism of how QQc restores the vasculogenic dysfunction of diabetic EPCs. We recently have looked into the effect of QQc on oxidative stress of control and diabetic BM KSL cells and found that QQc relieves oxidative stress on both control and diabetic BM KSL cells (data not shown). However, this was not the specific mechanism for restoring diabetic BM KSL dysfunction. We plan to investigate further in a future study.

In summary, we have demonstrated that QQc not only restores diabetic EPC function but also achieves supraphysiologic EPC vasculogenic function in vitro and in vivo. Because QQc is serum-free and rapidly expands the number of diabetic EPCs, this system may facilitate cell-based therapies for diabetic patients. Although this study has limitations regarding future clinical applications for diabetic patients, this study can be considered the first step in establishing an ideal cell-based therapy for diabetic patients. Moreover, the rapidly expanded post-QQc EPC population could be aliquoted, cryopreserved, and used again for metachronous wounds or other ischemic conditions (e.g., myocardial ischemia).

Conclusions. Here, we demonstrate that a novel serum-free QQc system expands the number of cells and enhances the vasculogenic and therapeutic potential of diabetic EPCs. We hypothesize that adoptive post-QQc diabetic EPC therapy may be an effective cell-based therapy for nonhealing diabetic wounds.

ACKNOWLEDGMENTS

This work was supported by a Health and Labor Sciences research grant from the Japanese Ministry of Health, Labor, and Welfare (20890227, 22791737), a funding program for Next Generation World Leading Researchers LS113, a Tokai University research aid grant, and Plastic Surgery Research Award 2007 (awarded to R.T.).

No potential conflicts of interest relevant to this article were reported.

R.T. conceived and designed the study, obtained financial support, wrote the manuscript, provided the study

material, collected data, analyzed data, and interpreted data. M.V. collected data, analyzed data, interpreted data, and wrote the manuscript. H.M. conceived and designed the study and wrote the manuscript. R.I. collected and assembled data, analyzed data, and interpreted data. M.K. collected data, assembled data, analyzed data, and interpreted data. M.M. provided administrative support. H.M. wrote the manuscript. S.M.W. obtained financial support, provided administrative support, wrote the manuscript, and approved the final manuscript. T.A. obtained financial support, provided administrative support, wrote the manuscript, and approved the final manuscript. T.A. is the guarantor of this work and, as such, had full access to all of the data in the study and takes responsibility for the integrity of the data and the accuracy of the data analysis.

The authors acknowledge the contributions of Christopher C. Chang, Dan Bassiri, Clarence Lin, Oren M. Tepper, and Anthony L. Rios (all from Institute of Reconstructive Plastic Surgery Laboratories, Department of Plastic Surgery, New York University Medical Center, New York, New York), Mika Wada (from Tokai University School of Medicine, Department of Regenerative Medicine), and Satoshi Fujimura, Kayo Okada, and Kayoko Arita (from Juntendo University School of Medicine, Department of Plastic and Reconstructive Surgery) for their kind technical assistance. The authors also thank Dr. Yoshinori Okada, Dr. Hiroshi Kamiguchi, and Yoko Kameyama (from Tokai University School of Medicine) for their outstanding technical support regarding flow cytometry, real-time PCR, and immunohistochemistry.

REFERENCES

1. Drake CJ. Embryonic and adult vasculogenesis. Birth Defects Res C Embryo Today 2003;69:73–82
2. Asahara T, Murohara T, Sullivan A, et al. Isolation of putative progenitor endothelial cells for angiogenesis. Science 1997;275:964–967
3. Shi Q, Rafii S, Wu MH, et al. Evidence for circulating bone marrow-derived endothelial cells. Blood 1998;92:362–367
4. Hristov M, Erl W, Weber PC. Endothelial progenitor cells: isolation and characterization. Trends Cardiovasc Med 2003;13:201–206
5. Tanaka R, Wada M, Kwon SM, et al. The effects of flap ischemia on normal and diabetic progenitor cell function. Plast Reconstr Surg 2008;121:1929–1942
6. Kwon SM, Lee YK, Yokoyama A, et al. Differential activity of bone marrow hematopoietic stem cell subpopulations for EPC development and ischemic neovascularization. J Mol Cell Cardiol 2011;51:308–317
7. Asahara T, Masuda H, Takahashi T, et al. Bone marrow origin of endothelial progenitor cells responsible for postnatal vasculogenesis in physiological and pathological neovascularization. Circ Res 1999;85:221–228
8. Tepper OM, Capla JM, Galiano RD, et al. Adult vasculogenesis occurs through in situ recruitment, proliferation, and tubulization of circulating bone marrow-derived cells. Blood 2005;105:1068–1077
9. Ii M, Nishimura H, Iwakura A, et al. Endothelial progenitor cells are rapidly recruited to myocardium and mediate protective effect of ischemic preconditioning via "imported" nitric oxide synthase activity. Circulation 2005;111:1114–1120
10. Ceradini DJ, Kulkarni AR, Callaghan MJ, et al. Progenitor cell trafficking is regulated by hypoxic gradients through HIF-1 induction of SDF-1. Nat Med 2004;10:858–864
11. Murayama T, Tepper OM, Silver M, et al. Determination of bone marrow-derived endothelial progenitor cell significance in angiogenic growth factor-induced neovascularization in vivo. Exp Hematol 2002;30:967–972
12. Tepper OM, Carr J, Allen RJ Jr, et al. Decreased circulating progenitor cell number and failed mechanisms of stromal cell-derived factor-1alpha mediated bone marrow mobilization impair diabetic tissue repair. Diabetes 2010;59:1974–1983
13. Schatteman GC, Hanlon HD, Jiao C, Dodds SG, Christy BA. Blood-derived angioblasts accelerate blood-flow restoration in diabetic mice. J Clin Invest 2000;106:571–578
14. Loomans CJ, de Koning EJ, Staal FJ, et al. Endothelial progenitor cell dysfunction: a novel concept in the pathogenesis of vascular complications of type 1 diabetes. Diabetes 2004;53:195–199
15. Li Calzi S, Neu MB, Shaw LC, Grant MB. Endothelial progenitor dysfunction in the pathogenesis of diabetic retinopathy: treatment concept to correct diabetes-associated deficits. EPMA J 2010;1:88-100
16. Albiero M, Menegazzo L, Boscaro E, Agostini C, Avogaro A, Fadini GP. Defective recruitment, survival and proliferation of bone marrow-derived progenitor cells at sites of delayed diabetic wound healing in mice. Diabetologia 2011;54:945–953
17. Fadini GP, Sartore S, Albiero M, et al. Number and function of endothelial progenitor cells as a marker of severity for diabetic vasculopathy. Arterioscler Thromb Vasc Biol 2006;26:2140–2146
18. Neukomm LJ, Frei AP, Cabello J, et al. Loss of the RhoGAP SRGP-1 promotes the clearance of dead and injured cells in Caenorhabditis elegans. Nat Cell Biol 2011;13:79–86
19. Kawamoto A, Gwon HC, Iwaguro H, et al. Therapeutic potential of ex vivo expanded endothelial progenitor cells for myocardial ischemia. Circulation 2001;103:634–637
20. Kocher AA, Schuster MD, Szabolcs MJ, et al. Neovascularization of ischemic myocardium by human bone-marrow-derived angioblasts prevents cardiomyocyte apoptosis, reduces remodeling and improves cardiac function. Nat Med 2001;7:430–436
21. Taguchi A, Soma T, Tanaka H, et al. Administration of CD34+ cells after stroke enhances neurogenesis via angiogenesis in a mouse model. J Clin Invest 2004;114:330–338
22. Lin CD, Allori AC, Macklin JE, et al. Topical lineage-negative progenitor-cell therapy for diabetic wounds. Plast Reconstr Surg 2008;122:1341–1351
23. Sivan-Loukianova E, Awad OA, Stepanovic V, Bickenbach J, Schatteman GC. CD34+ blood cells accelerate vascularization and healing of diabetic mouse skin wounds. J Vasc Res 2003;40:368–377
24. Tanaka R, Masuda H, Kato S, et al. Autologous G-CSF mobilized peripheral blood CD34(+) cell therapy for diabetic patients with chronic non-healing ulcer. Cell Transplant. 25 October 2012 [Epub ahead of print]
25. Jarajapu YP, Grant MB. The promise of cell-based therapies for diabetic complications: challenges and solutions. Circ Res 2010;106:854–869
26. Tan Q, Qiu L, Li G, et al. Transplantation of healthy but not diabetic outgrowth endothelial cells could rescue ischemic myocardium in diabetic rabbits. Scand J Clin Lab Invest 2010;70:313–321
27. Masuda H, Iwasaki H, Kawamoto A, et al. Development of serum-free quality and quantity control culture of colony-forming endothelial progenitor cell for vasculogenesis. Stem Cells Transl Med 2012;1:160–171
28. Westermann D, Rutschow S, Van Linthout S, et al. Inhibition of p38 mitogen-activated protein kinase attenuates left ventricular dysfunction by mediating pro-inflammatory cardiac cytokine levels in a mouse model of diabetes mellitus. Diabetologia 2006;49:2507–2513
29. Masuda H, Alev C, Akimaru H, et al. Methodological development of a clonogenic assay to determine endothelial progenitor cell potential. Circ Res 2011;109:20–37
30. Tanaka R, Wada M, Kwon S, et al. The effects of flap ischemia on normal and diabetic progenitor cell function. Plast Reconstr Surg 2008;121:1929–1942
31. Park S, Tepper OM, Galiano RD, et al. Selective recruitment of endothelial progenitor cells to ischemic tissues with increased neovascularization. Plast Reconstr Surg 2004;113:284–293
32. Pugazhenthi K, Kapoor M, Clarkson AN, Hall I, Appleton I. Melatonin accelerates the process of wound repair in full-thickness incisional wounds. J Pineal Res 2008;44:387–396
33. Carson FL. *Histotechnology: A Self-Instructional Text.* Chicago, ASCP Press, 1997
34. Fadini GP, Avogaro A. Potential manipulation of endothelial progenitor cells in diabetes and its complications. Diabetes Obes Metab 2010;12:570–583
35. Michaels J, Churgin SS, Blechman KM, Greives MR, Aarabi S, Galiano RD, Gurtner GC. db/db mice exhibit severe wound-healing impairments compared with other murine diabetic strains in a silicone-splinted excisional wound model. Wound Repair Regen 2007;15:665–670
36. Glotzbach JP, Levi B, Wong VW, Longaker MT, Gurtner GC. The basic science of vascular biology: implications for the practicing surgeon. Plast Reconstr Surg 2010;126:1528–1538
37. King SJ, Worth DC, Scales TM, Monypenny J, Jones GE, Parsons M. β1 integrins regulate fibroblast chemotaxis through control of N-WASP stability. EMBO J 2011;30:1705–1718
38. Bakker K, Apelqvist J, Schaper NC; International Working Group on Diabetic Foot Editorial Board. Practical guidelines on the management and prevention of the diabetic foot 2011. Diabetes Metab Res Rev 2012;28 (Suppl. 1):225–231

Circulation
JOURNAL OF THE AMERICAN HEART ASSOCIATION

American Heart Association®

Enhanced Survival of Transplanted Human Induced Pluripotent Stem Cell–Derived Cardiomyocytes by the Combination of Cell Sheets With the Pedicled Omental Flap Technique in a Porcine Heart

Masashi Kawamura, Shigeru Miyagawa, Satsuki Fukushima, Atsuhiro Saito, Kenji Miki, Emiko Ito, Nagako Sougawa, Takuji Kawamura, Takashi Daimon, Tatsuya Shimizu, Teruo Okano, Koichi Toda and Yoshiki Sawa

Circulation. 2013;128:S87-S94
doi: 10.1161/CIRCULATIONAHA.112.000366
Circulation is published by the American Heart Association, 7272 Greenville Avenue, Dallas, TX 75231

Print ISSN: 0009-7322. Online ISSN: 1524-4539

Enhanced Survival of Transplanted Human Induced Pluripotent Stem Cell–Derived Cardiomyocytes by the Combination of Cell Sheets With the Pedicled Omental Flap Technique in a Porcine Heart

Masashi Kawamura, MD; Shigeru Miyagawa, MD, PhD; Satsuki Fukushima, MD, PhD; Atsuhiro Saito, PhD; Kenji Miki, PhD; Emiko Ito, PhD; Nagako Sougawa, PhD; Takuji Kawamura, MD; Takashi Daimon, PhD; Tatsuya Shimizu, MD, PhD; Teruo Okano, PhD; Koichi Toda, MD, PhD; Yoshiki Sawa, MD, PhD

Background—Transplantation of cardiomyocytes that are derived from human induced pluripotent stem cell–derived cardiomyocytes (hiPS-CMs) shows promise in generating new functional myocardium in situ, whereas the survival and functionality of the transplanted cells are critical in considering this therapeutic impact. Cell-sheet method has been used to transplant many functional cells; however, potential ischemia might limit cell survival. The omentum, which is known to have rich vasculature, is expected to be a source of blood supply. We hypothesized that transplantation of hiPS-CM cell sheets combined with an omentum flap may deliver a large number of functional hiPS-CMs with enhanced blood supply.

Methods and Results—Retrovirally established human iPS cells were treated with Wnt signaling molecules to induce cardiomyogenic differentiation, followed by superparamagnetic iron oxide labeling. Cell sheets were created from the magnetically labeled hiPS-CMs using temperature-responsive dishes and transplanted to porcine hearts with or without the omentum flap (n=8 each). Two months after transplantation, the survival of superparamagnetic iron oxide–labeled hiPS-CMs, assessed by MRI, was significantly greater in mini-pigs with the omentum than in those without it; histologically, vascular density in the transplanted area was significantly greater in mini-pigs with the omentum than in those without it. The transplanted tissues contained abundant cardiac troponin T–positive cells surrounded by vascular-rich structures.

Conclusions—The omentum flap enhanced the survival of hiPS-CMs after transplantation via increased angiogenesis, suggesting that this strategy is useful in clinical settings. The combination of hiPS-CMs and the omentum flap may be a promising technique for the development of tissue-engineered vascular-rich new myocardium in vivo. **(*Circulation*. 2013;128[suppl 1]:S87-S94.)**

Key Words: cell transplantation ■ induced pluripotent stem cells ■ regeneration

Stem cell therapy shows promise in the treatment of heart failure. However, the therapeutic benefits proven by clinical studies in the past decade were only modest, indicating that further investigations and refinements are required to establish this treatment in the clinical arena.[1,2] The success of cell transplantation therapy for heart failure is dependent on the choice of cell source, cell delivery method, and target cardiac pathology. In these previous clinical trials, transplantation of somatic tissue–derived stem or progenitor cells has shown no or low cardiomyogenic differentiation capacity in vivo, but contributed to functional recovery via paracrine effects, potentially limiting the therapeutic effects, in particular, in treating severe heart failure.[1–4] In addition, it has been shown that direct intramyocardial or intracoronary injection of dissociated single cells, which was used in most of the clinical studies, yields <10% of engraftment rate of the cells immediately after transplantation, indicating that further refinement of the cell delivery method would be required to increase cell engraftment and enhance the consequent therapeutic effects.[1,2]

Human induced pluripotent stem (hiPS) cells are initially established by nuclear reprogramming of somatic cells.[5,6] hiPS cell carries a capacity of unlimited proliferation and differentiation to cardiomyocyte.[7] Transplantation of hiPS-derived cardiomyocytes (hiPS-CMs) would have, thus, a potential to

From the Department of Cardiovascular Surgery, Osaka University Graduate School of Medicine, Suita, Osaka, Japan (M.K., S.M., S.F., K.M., E.I., N.S., T.K., K.T., Y.S.); Medical Center for Translational Research, Osaka University Hospital, Suita, Osaka, Japan (A.S.); Department of Biostatistics, Hyogo College of Medicine, Nishinomiya, Hyogo, Japan (T.D.); Institute of Advanced Biomedical Engineering and Science, Tokyo Women's Medical University, Tokyo, Japan (T.S., T.O.).

Presented at the 2012 American Heart Association meeting in Los Angeles, CA, November 3–7, 2012.

The online-only Data Supplement is available with this article at http://circ.ahajournals.org/lookup/suppl/doi:10.1161/CIRCULATIONAHA.112.000366/-/DC1.

Correspondence to Yoshiki Sawa, MD, PhD, Department of Cardiovascular Surgery, Osaka University Graduate School of Medicine, 2-2(E1) Yamadaoka, Suita, Osaka 565-0871, Japan. E-mail sawa-p@surg1.med.osaka-u.ac.jp

Circulation **is available at http://circ.ahajournals.org** **DOI: 10.1161/CIRCULATIONAHA.112.000366**

increase the functional cardiomyocytes in damaged heart tissue to mechanically contribute to cardiac function. In addition, the recently developed scaffoldless tissue engineering technique of cell-sheet engineering is applicable to myocardial regeneration therapy.[8] This technique preserves extracellular matrix without artificial scaffolds, which may prevent cell detachment–associated anoikis.[9] In contrast to the needle injection technique, the cell-sheet technique can deliver a large number of cells to the damaged myocardium without loss of transplanted cells or injury to the host myocardium.[10,11] Importantly, this method has already shown feasibility and safety in the clinical study.[12] On these bases, we studied the therapeutic efficacy of transplantation of hiPS-CMs with the cell-sheet method in a porcine chronic ischemic cardiomyopathy model.[13] This study, however, showed that the transplanted cells rarely survived in the heart long-term, possibly because of poor vascular network support from the native tissue.

The omentum has been historically used in surgical revascularization for patients with ischemic heart disease[14–16] and is also known to have rich vasculature and angiogenic factors.[17,18] Importantly, we reported that a pedicle omentum flap covering the transplanted skeletal myoblast cell sheets enhanced angiogenesis over the cell-sheet–transplanted territory, survival of cells, and therapeutic effects.[19] We herein hypothesized that covering with an omentum flap may enhance the survival of transplanted hiPS-CM cell sheets via the promotion of angiogenesis over the transplanted territory. In this study, we compared the survival of hiPS-CMs, with or without a pedicle omentum flap, after transplantation to the mini-pig heart, and we examined whether the omentum enhanced the angiogenic capacity of hiPS-CM sheets in vivo.

Materials and Methods

All experimental procedures were approved by the institutional ethics committee. Animal care was conducted humanely in compliance with the Principles of Laboratory Animal Care formulated by the National Society for Medical Research and the Guide for the Care and Use of Laboratory Animals prepared by the Institute of Animal Resources and published by the National Institutes of Health (publication no. 85-23, revised 1996).

Preparation of SPIO-Labeled hiPS-CM Cell Sheets

The hiPS cell line 201B7 that was generated using the 4 transcription factors Oct4, Sox2, Klf4, and c-Myc was used in this study.[5] Culture of the hiPS cells, formation of the embryoid bodies, and subsequent cardiomyogenic differentiation and purification were performed as described previously to generate hiPS-CMs.[13] The purified hiPS-CMs were then labeled with the superparamagnetic iron oxide (SPIO) ferucarbotran (Resovist; Bayer Pharma, Berlin, Germany) using the hemagglutinating virus of Japan envelope vector (GenomOne-Neo; Ishihara Sangyo, Osaka, Japan).[20,21] Subsequently, human mesenchymal stem cells (Lonza, Basel, Switzerland) were seeded at a density of 5×10^6 cells/dish onto 10-cm UpCell dishes, on which the SPIO-labeled hiPS-CMs were grown. The next day, the dishes were incubated at room temperature, which induced the cells to detach spontaneously to form scaffold-free hiPS-CM cell sheets.

Flow Cytometry

Dissociated cells after hiPS cell differentiation were fixed, permeabilized, and labeled with anticardiac isoform of troponin T (cTNT; clone 13211; Thermo Fisher scientific, Runcorn, UK) conjugated with Alexa-488 using Zenon technology (Invitrogen), followed by analysis on BD FACSCanto II (BD Biosciences) with BD FACSDiva Software (BD Biosciences).

Study Protocol

Normal 16 female mini-pigs (Japan Farm Co Ltd, Kagoshima, Japan) weighing 20 to 25 kg were randomly divided into 2 groups (n=8 each) to perform hiPS-CM cell-sheet transplantation either with or without the pedicle omentum translocation. All animals were immunosuppressed by daily administration of tacrolimus (0.75 mg/kg; Astellas, Tokyo, Japan), mycophenolate mofetil (500 mg; Teva Czech Industries s.r.o, Opava, Czech), and prednisolone (20 mg; Takeda Pharmaceutical Co Ltd, Osaka, Japan) daily from 5 days before transplantation until euthanasia. Cardiac MRI scans were taken on the same mini-pigs at 1 week, 4 weeks, and 8 weeks after transplantation. After the final scan, the mini-pigs were humanely euthanized for analysis (Figure 1A).

Transplantation of SPIO-Labeled hiPS-CM Cell Sheets Covered With the Pedicle Omentum

All animals were preanesthetized with ketamine hydrochloride (20 mg/kg; Daiichi Sankyo, Tokyo, Japan) and xylazine (2 mg/kg; Bayer HealthCare, Leverkusen, Germany), intubated endotracheally, and maintained by continuous infusion of propofol (6 mg/kg per hour; AstraZeneca K.K., Osaka, Japan) and vecuronium bromide (0.05 mg/kg per hour; Daiichi Sankyo). Seven SPIO-labeled hiPS-CM sheets were placed on the epicardium via the median sternotomy. In the case of transplantation of the cell sheet covered with the pedicled omentum, the omentum was mobilized to the mediastinal space via additional small upper midline laparotomy, preserving both gastroepiploic arteries and their arcade. Initially, 4 hiPS-CM cell sheets were placed on the epicardium and covered with the omentum. The remaining 3 hiPS-CM cell sheets, then, were placed on the covering omentum and covered with the omentum again (Figure 1B). The omentum was stitched and fixed on the excised pericardium (Figure 1C). Mini-pigs were then allowed to recover and were later humanely euthanized.

Cardiac MRI

ECG-gated cardiac MRI (CMR) was performed under general anesthesia with an 8-channel cardiac coil wrapped around the chest wall.[22] CMR images were acquired on a 1.5-T MR scanner (Signa EXCITE XI TwinSpeed; GE Medical Systems, Milwaukee, WI). To assess SPIO-labeled hiPS-CM detection, animals were imaged 1 week after transplantation. In addition, 1 animal was reimaged at 4 and 8 weeks after transplantation to detect SPIO-labeled hiPS-CM retention. Short-axis images with 8-mm slice thickness, including the entire heart, were obtained by pulse parameters for cardiac-gated, fast gradient–recalled echo. The SPIO-labeled hiPS-CM hypointense area was measured using planimetry of fast gradient–recalled echo images on a workstation (Virtual Place Lexus64; AZE, Tokyo, Japan). The survival proportion of hiPS-CMs was determined using the hypointense area at 4 and 8 weeks after transplantation divided by the area at 1 week after transplantation as the baseline.

Histology and Immunohistolabeling

The hiPS-CM cell sheets and the excised heart specimens were either embedded in paraffin or optimal cutting temperature compound (Tissueb Tek; Sakura Finetek, Torrance, CA) for frozen section. The paraffin-embedded sections were stained with hematoxylin–eosin or Prussian blue that visualizes iron contents. Ten different fields were randomly selected. The number of spindle-shaped cells with a nucleus and iron in the cytoplasm in each field was counted with a light microscopy under high-power magnification (×400). Cells from 10 fields were averaged, and the results are expressed as cell density (per high-power field). In addition, the paraffin-embedded sections were immunolabeled with anti-human von Willebrand factor antibody (Dako, Glostrup, Denmark) and visualized with the horseradish peroxidase-based EnVision kit (Dako). Ten different fields were randomly selected, and the number of von Willebrand factor–positive

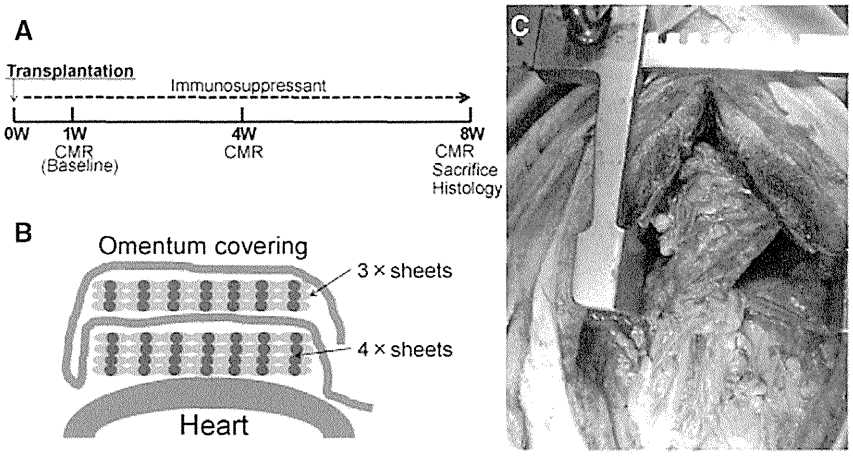

Figure 1. Study protocol of the mini-pig experiment and operative procedure. **A**, Schedule of cardiac MRI (CMR) and histological evaluations. **B**, Procedural scheme of cell-sheet transplantation with the omentum. **C**, Image taken after treatment. The omentum is mobilized and transplanted with the cell sheets on the heart through median sternotomy with an additional upper midline laparotomy.

cells in each field was counted using a light microscope under high-power magnification (×200). The stained blood vessels from the 10 fields were averaged and the results expressed as vascular density (per square millimeter). The frozen sections were immunolabeled with anti-cTNT antibody (1:100 dilution; Abcam, Cambridge, UK) and anti-CD68 antibody for macrophages (1:100 dilution, Abcam) as primary antibodies and visualized with AlexaFluor488–conjugated goat anti-mouse (Invitrogen) and AlexaFluor555–conjugated goat anti-rabbit (Invitrogen) as secondary antibodies. Nuclei were counterstained with 4′,6-diamidino-2-phenylindole (Dojindo, Tokyo, Japan) and assessed using the Biorevo BZ-9000 (Keyence) or confocal microscopy (Olympus Japan, FV1000-D IX81, Tokyo, Japan). SPIO particles of Prussian blue staining were visualized by differential interference contrast of confocal microscopy.

Real-Time Polymerase Chain Reaction

Total RNA was extracted from cardiac tissue and reverse transcribed using Omniscript reverse transcriptase (Qiagen, Hilden, Germany) with random primers (Invitrogen), and the resulting cDNA was used for real-time polymerase chain reaction with the ABI PRISM 7700 (Applied Biosystems, Stockholm, Sweden) system using pig-specific primers (Applied Biosystems) for vascular endothelial growth factor (VEGF), basic fibroblast growth factor, and stromal-derived factor-1 (SDF-1). Each sample was analyzed in triplicate for each gene studied. Data were normalized to GAPDH expression level. For relative expression analysis, the delta-delta Ct method was used, and values of the cell-sheet transplantation without the omentum were used as reference values.

Statistical Analysis

Data are expressed as means±SDs. Comparisons between 2 groups were made using Welch t test. Cell survival proportion over time was assessed by repeated-measures ANOVA with group, time, and group×time interaction effects. All P values are 2-sided, and values of $P<0.05$ were considered to indicate statistical significance. Statistical analyses were performed using JMP 9.02 (SAS Institute, Cary, NC).

Results

Generation of SPIO-Labeled hiPS-CM Cell Sheets

Cardiomyogenic differentiation of hiPS cells was induced by treatment of the embryoid bodies formed from cultured hiPS cells with Wnt3a and R-spondin-1. Subsequently, the differentiated hiPS cells were purified by culture in glucose-free medium to yield ≈1 to 2×10^7 hiPS-CMs. Approximately 80% (83.6±8.1%) of the hiPS-CMs were positive for cTNT, as determined by flow cytometry (Figure 2A). After SPIO labeling to the hiPS-CMs, human mesenchymal stem cells were added to the hiPS-CM culture. Subsequently, culture in the thermo-responsive dishes yielded round-shaped hiPS-CM cell sheets (Figure 2B). The hiPS-CMs on the sheet continued to beat before and after detaching from culture surface (Movies I and II in the online-only Data Supplement). Immunohistolabeling showed that the large number of cells in the hiPS-CM cell sheets were homogeneously positive for cTNT (Figure 2C). Prussian blue staining confirmed that the hiPS-CMs contained iron in the cytoplasm (Figure 2D).

In Vivo Analysis of Survival of Transplanted SPIO-Labeled hiPS-CMs by Serial CMR

Transplantation of the same number of hiPS-CM cell sheets with or without the omentum covering was successfully performed via median sternotomy in 16 normal mini-pigs. There was no mortality related to the procedure or otherwise before the planned euthanasia. In addition, the omentum was attached to the surface of the heart in all mini-pigs with the omentum. CMRs were performed to assess the survival of transplanted SPIO-labeled hiPS-CMs at 1 week (baseline), 4 weeks, and 8 weeks after cell transplantation.

SPIO signals were clearly identified as the hypointense area in the surface of the left ventricle by CMR in all mini-pigs throughout the study period (Figure 3A). SPIO-positive hypointense area was gradually decreased in both the groups during the 8 weeks, whereas the SPIO-positive area was larger and thicker in mini-pigs with the omentum compared with those without the omentum during the study period. The survival proportion of the SPIO-labeled hiPS-CMs was determined by the formula that the hypointense area at 4 and 8 weeks after transplantation was divided by the area at 1 week after transplantation as baseline. Both groups showed steady decrease in the cell survival during the 7 weeks, whereas the proportion of decrease was significantly less in mini-pigs with the omentum than in those without it at 4 weeks (92±10% versus 60±10%) and 8 weeks (78±10% versus 42±9%) after treatment ($P<0.0001$ for interaction effect of time and group in the repeated ANOVA; Figure 3B).

Histological Evaluation of Transplanted hiPS-CMs With or Without the Omentum

Excised heart tissues at 8 weeks after transplantation were assessed by histology. The transplanted hiPS-CMs and the

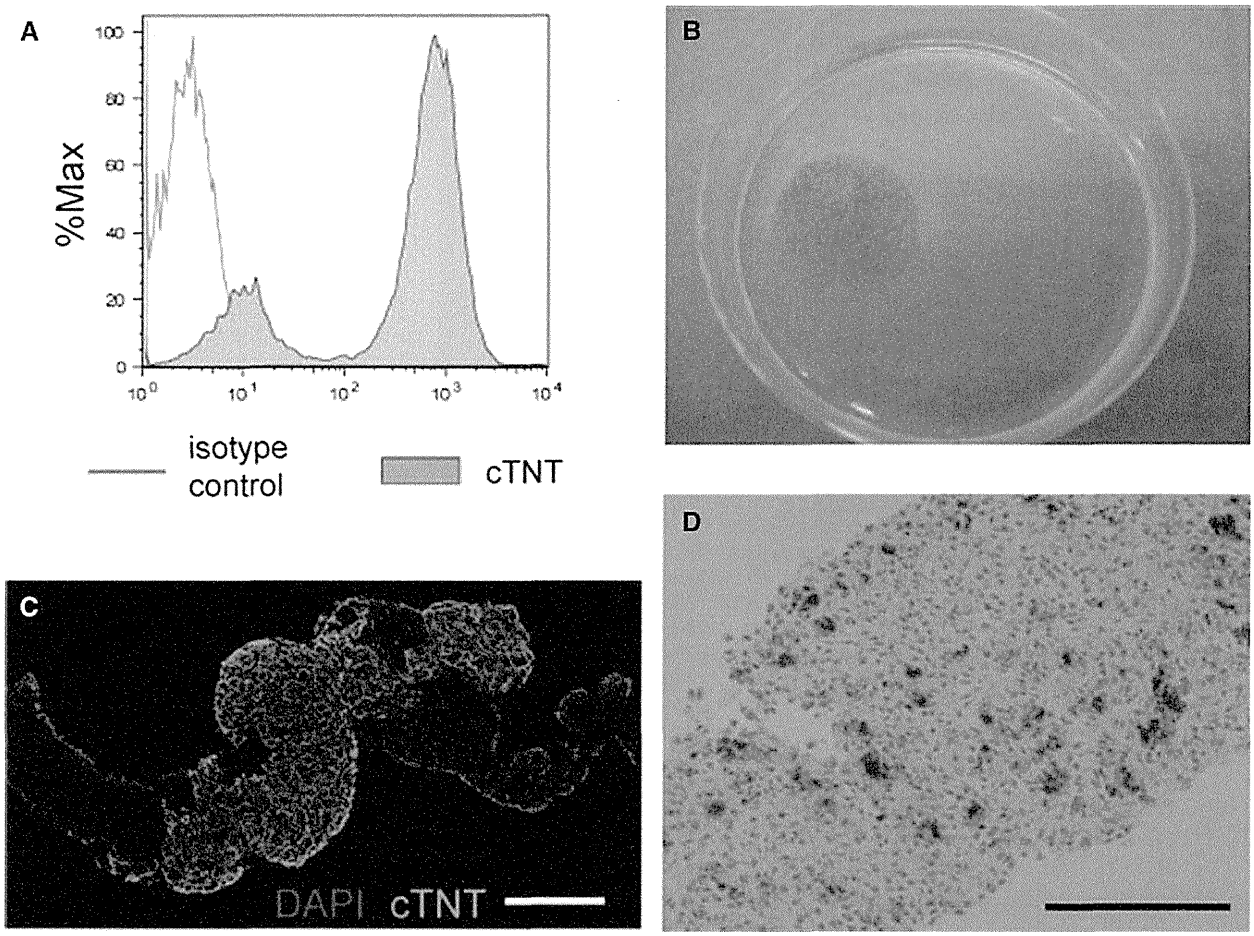

Figure 2. Histological characteristics of the human induced pluripotent stem cell–derived cardiomyocyte (hiPS-CM) cell sheet. **A**, Expression of cardiac troponin T (cTNT) after differentiation and purification of hiPS-CMs. **B**, A superparamagnetic iron oxide (SPIO)–labeled hiPS-CM cell sheet in a 10-cm dish. **C**, Immunostaining of the hiPS-CM cell sheet with cTNT antibody (green). The cell nuclei were counterstained with 4′,6-diamidino-2-phenylindole (DAPI; blue). **D**, Prussian blue staining of the SPIO-labeled hiPS-CM cell sheet. Scale bar, 50 μm in **C** and **D**.

pedicle omentum were attached over the epicardium of the left ventricle without any histological gaps in all mini-pigs, as assessed by hematoxylin–eosin staining (Figure 4D). The hearts without the omentum showed cellular and fibrous components over the anterior wall of the ventricles (Figure 4A), whereas the hearts with the omentum showed thick cellular, fibrous, and fat-rich components covering the anterior and lateral wall of the ventricles (Figure 4D).

Prussian blue staining revealed cells containing iron on the surface of the ventricles, corresponding to the area seen on CMR in both groups (Figure 4B and 4E). A larger number of cells with iron contents were identified in mini-pigs with the omentum compared with those without (Figure 4B, 4C, 4E, and 4F). In fact, the density of iron-containing cells in the transplanted site, assessed semiquantitatively by Prussian blue staining at 8 weeks after treatment, was significantly greater in the mini-pig with the omentum (27±6 cells/high-power field) than in those without it (5±2 cells/high-power field; $P<0.0001$; Figure 4G). Immunohistolabeling showed that a larger number of cells are positive for cTNT in the area where cells with iron inclusions are present in mini-pigs with the omentum compared with those without it (Figure 4H). The distribution of the SPIO particles was visualized by differential interference contrast of confocal microscopy. Grafted hiPS-CMs were identified and confirmed as double-positive for cTNT and SPIO and negative for CD68, which is a specific marker for macrophages, by immunohistolabeling (Figure 4I–4N). In addition, no teratomas were formed in the heart or other thoracic organs at 8 weeks after the transplantation of the hiPS-CM cell sheets with or without the omentum (data not shown).

Capillary Density in the Transplanted Area

Vessels and capillaries in the transplanted cell sheets at 8 weeks after transplantation were visualized and assessed by immunohistochemistry for von Willebrand factor. The transplanted cell sheets without the omentum contained a large number of capillaries and a small number of vessels in a homogeneous manner (Figure 5A), suggesting that vascular network was created possibly to support the survival and function of the cell sheets. Of note, the number of capillaries and vessels were markedly greater in the cell sheets covered by the omentum compared with those without it (Figure 5B). In fact, capillary density in the transplanted cell sheets, assessed semiquantitatively by immunohistochemistry for von Willebrand factor at 8 weeks after treatment, was significantly and markedly

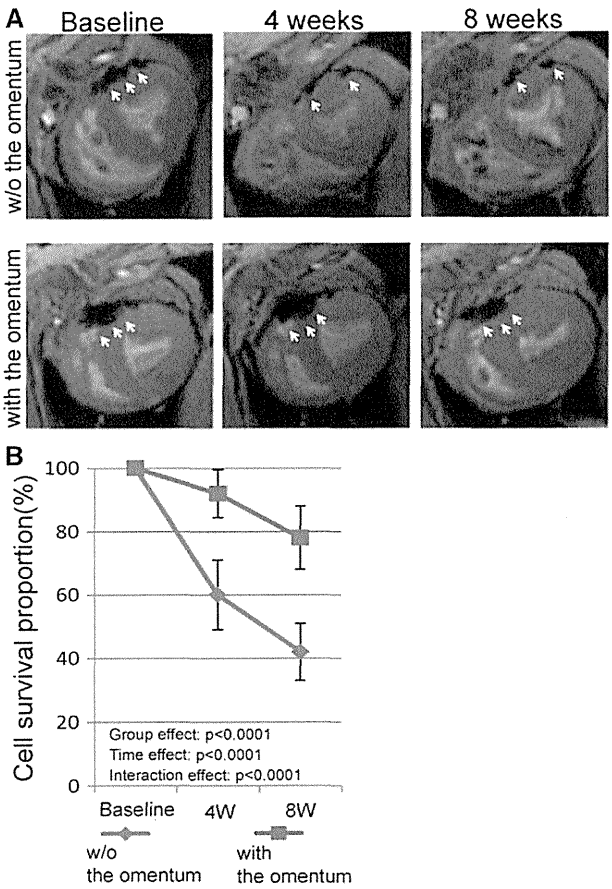

Figure 3. In vivo analysis of the survival of superparamagnetic iron oxide (SPIO)–labeled human induced pluripotent stem cell–derived cardiomyocytes (hiPS-CMs) after transplantation. **A**, Serial cardiac MRIs were examined at 1 week (baseline), 4 weeks, and 8 weeks after SPIO-labeled hiPS-CM cell-sheet transplantation, with or without the omentum. Representative hypointense area of the SPIO-labeled hiPS-CMs is indicated by white arrows. **B**, Cell survival proportion was estimated by the SPIO-labeled area at 4 and 8 weeks, corrected by cell survival at 1 week.

greater in mini-pigs with the omentum (64±21 U/mm^2) than in those without it (9±5 U/mm^2; P<0.0001; Figure 5C).

Upregulation of VEGF, Basic Fibroblast Growth Factor, and SDF-1 Expression in the Transplanted Area

The expression level of cardioprotective and angiogenic factors in the transplanted area at 8 weeks after treatment was quantitatively assessed by real-time polymerase chain reaction for VEGF, basic fibroblast growth factor, and SDF-1. The relative expression of all the factors in the transplanted area was significantly greater in mini-pigs with the omentum than in those without it (VEGF, 1.94±0.38 versus 1.35±0.26; P<0.05; basic fibroblast growth factor, 2.33±0.92 versus 1.21±0.19; P<0.05; SDF-1, 2.05±0.33 versus 1.22±0.21; P<0.01; Figure 6A–6C).

Discussion

It is herein demonstrated that our differentiation protocol yielded hiPS-CMs with >80% purity, and hiPS-CM cell sheets were transplanted over the anterior wall of the ventricle, covered by the pedicle omentum, in a porcine model without procedural failure or procedure-related morbidity/mortality. The number of surviving cTNT-positive hiPS-CMs on the native myocardium was significantly greater in mini-pigs with the omentum than in those without it, although there was a steady decrease in the surviving cell number, regardless of the omentum support, as assessed by SPIO cell labeling with CMR and by immunohistolabeling. The pedicle omentum covering markedly increases the number of vessels and capillaries, associated with the upregulation of VEGF, hepatocyte growth factor, and SDF-1, at the transplanted area compared with the cell-sheet transplantation without the omentum.

In the present study, SPIO-labeled hiPS-CMs were clearly visualized in vivo by CMR, corresponding to the histological findings that confirmed iron contents in the transplanted hiPS-CMs that were positive for cTNT, as reported by previous publications.[22,23] Using this method, the distribution and survival of the transplanted hiPS-CMs were serially evaluated in this study. As a result, it was proved that the unique technique in which transplanted cell sheets were covered by the pedicle omentum elicited a greater survival of the transplanted hiPS-CMs over the ventricular epicardial surface at 4 weeks compared with cell-sheet transplantation without the omentum covering. This suggests that pedicle omentum covering the cell sheets promptly induced angiogenesis to improve the hypoxic environment at the transplanted area, compared with the omentum-free method. In addition, although the size of the graft was decreased in both groups during the 8 weeks, trend in the size reduction was significantly milder in the omentum group than in the omentum-free group. This was consistent to the increased vascular network and upregulated angiogenic factors at the transplanted area in the omentum group at 8 weeks after the cell-sheet transplantation. These findings indicate that covering the cell sheet with the pedicle omentum that carries abundant angiogenic potentials[17–19] enhanced neovascular formation at the transplanted area promptly after transplantation and that vascular-rich structure at the transplanted area persisted long-term. In previous studies, antiapoptotic treatments on the transplanted cells, including upregulation of AKT[24] or overexpression of Bcl-2,[25] have been shown to improve survival after cell transplantation. We achieved to improve cell survival after transplantation by modifying the cell delivery method. The pedicled omental flap is frequently and safely applied for the treatment of mediastinitis after cardiovascular surgery. As cell transplantation is indicated to the patients with severe heart failure, we need to establish a minimally invasive approach to mobilize the omentum. Besides, we expect our unique combination method to be a feasible and safe treatment option in clinical settings. However, in this study, transplanted hiPS-CMs produced by our protocol may be immature, although they were spontaneously contractile. In the specimen 8 weeks after transplantation with the omentum, there were few surviving hiPS-CMs with organized sarcomeres in the cytoplasm, whereas there were many cTNT-positive cells (data not shown). In recent studies, mechanical load of hiPS-CMs in vitro controlled their alignment, proliferation, and hypertrophy,[26] and spontaneous and synchronous beating cardiac cell sheets were created by a bioreactor culture, which expanded and induced cardiac differentiation of hiPS cells.[27] It is necessary to modify

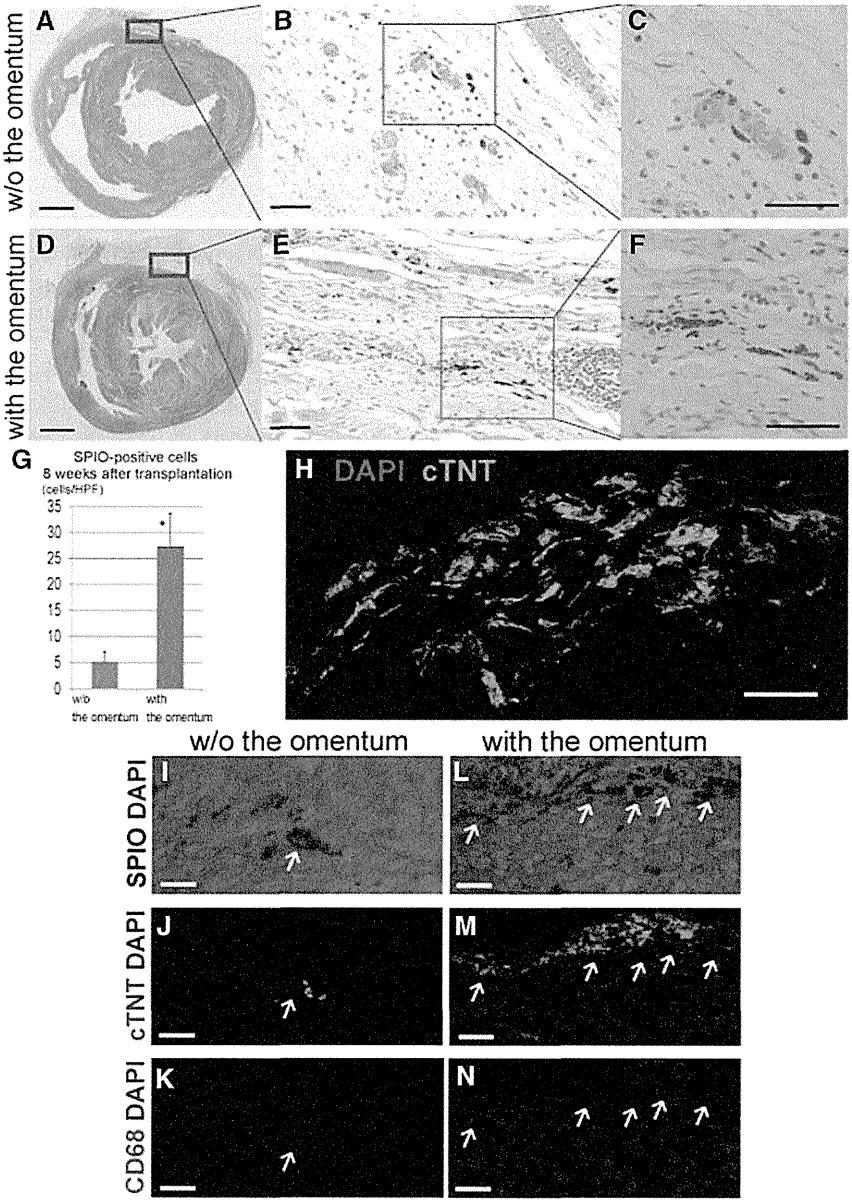

Figure 4. Human induced pluripotent stem cell–derived cardiomyocytes (hiPS-CMs) after transplantation. Macroscopic images of the whole heart by hematoxylin–eosin staining at the mid level in the mini-pig without (**A**) or with (**D**) the omentum; scale bar, 1 cm in **A** and **D**. Cells containing iron, indicative of superparamagnetic iron oxide (SPIO)–labeled hiPS-CMs, were detected by Prussian blue staining of sections of mini-pigs without (**B** and **C**) or with (**E** and **F**) the omentum at the transplanted area; scale bar, 50 μm in **B**, **C**, **E**, and **F**. **G**, The density of SPIO-positive cells in the transplanted site was semiquantitatively assessed at 8 weeks after treatment. *P<0.0001 vs without the omentum. **H**, In the transplanted regions of mini-pigs with the omentum, cardiac troponin T (cTNT)–positive cells were also demonstrated by immunohistolabeling (green). The cell nuclei were counterstained with 4′,6-diamidino-2-phenylindole (DAPI; blue); scale bar, 50 μm in **H**. **I**–**N**, In the transplanted regions of mini-pigs, SPIO particles were visualized by differential interference contrast (DIC), and grafted hiPS-CMs, which were double-positive for cTNT (green) and SPIO (DIC) and negative for CD68 (red), were indentified by immunohistolabeling. The cell nuclei were counterstained with DAPI (blue). Arrows indicate SPIO particles, referred to DIC images in **I** and **L**; scale bar, 20 μm in **I**–**N**.

our hiPS-CM preparation protocols referred to in these studies to yield the amount of contracting hiPS-CMs contributing to the mechanical function of the injured heart. In addition, we previously demonstrated that maturation of iPS-CMs progressed after iPS-CMs were transplanted in nude rat heart.[28] Therefore, we also expect that improving environments after cell transplantation, such as avoiding delivered cell ischemia, inflammation, and immunogenic rejection, will promote in vivo differentiation of iPS-CMs and their therapeutic effects. The combination of hiPS-CM sheets and the omentum is a promising delivery method to differentiate hiPS-CMs in vivo, because the omentum at least prevents cell ischemia after transplantation and provides better environments.

The cause of reduction in the graft size during the 8 weeks after the cell-sheet transplantation in both groups was not fully addressed in this study. However, one may consider that this reduction was caused by host immune rejection. We used a combined 3 immunosuppressant regimen, consisting of tacrolimus, mycophenolate mofetil, and corticosteroid, because our experiment was a xenotransplantation model, in which human tissue–derived cells were transplanted in a porcine. In addition, mesenchymal stem cells, which have the potential to induce immunologic tolerance,[29] were involved in creating hiPS-CM cell sheets, and recent studies have reported that the omentum has not only angiogenic cytokines and growth factors but also anti-inflammatory properties and thus can facilitate tissue healing of injured tissue or organs.[30] With our cell delivery method that combines the cell-sheet method with the pedicled omental flap, the 3-drug immunosuppressant regimen, and a mixture of mesenchymal stem cells, it would be difficult to permanently maintain a large number of delivered cells in this xenotransplantation model. Future clinical study of hiPS-CM transplantation for treating heart disease might be performed as allogeneic transplantation.[31] Further studies related to immunologic tolerance are needed to maintain the delivered cells long-term or permanently in this treatment.

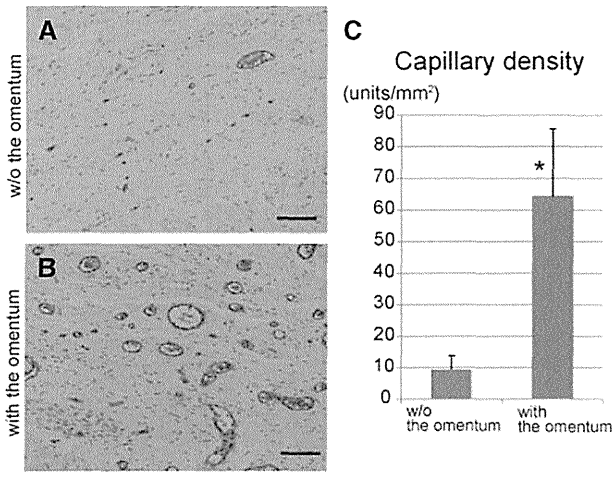

Figure 5. Capillary density in the transplanted area. Photomicrographs of immunostaining for von Willebrand factor are shown in **A** and **B**; scale bar, 50 μm. **C**, The capillary density in the transplanted area was significantly greater in the mini-pigs with the omentum than in those without it. *P<0.0001 vs without the omentum.

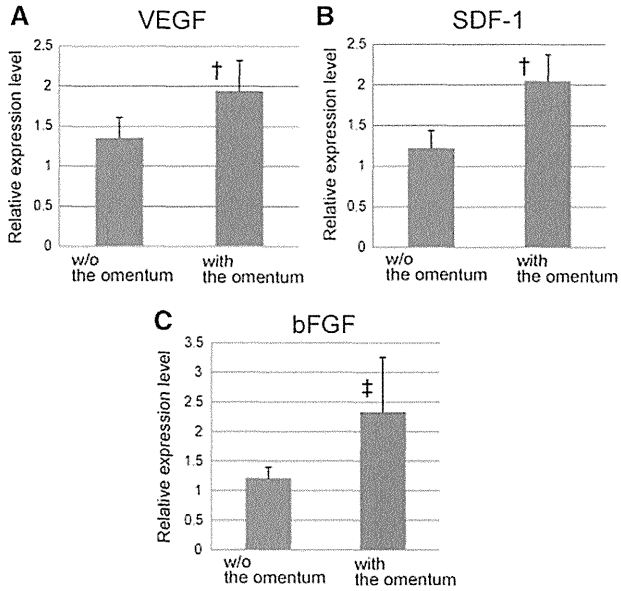

Figure 6. Angiogenesis-related mRNA expression in the transplanted area, as measured by real-time polymerase chain reaction. Relative expression of angiogenesis-related factors at the transplanted area was significantly greater in mini-pigs with the omentum than in those without it (**A**, vascular endothelial growth factor [VEGF], †P<0.05; **B**, stromal-derived factor [SDF]-1, †P<0.05; **C**, basic fibroblast growth factor [bFGF], ‡P<0.01 vs without the omentum).

In addition, more importantly, hiPS-CM cell sheets were transplanted over the normal epicardium, in which the tissue structure is well organized. New vascular network formation between the native myocardium and the transplanted cell sheets is thus insufficient to support the survival of the transplanted cells, leading to reduction of surviving transplanted cells long-term. In the clinical scenario, however, cell sheets will be transplanted over the diseased heart surface, in which epicardial structure is impaired. Conditions of the host myocardium possibly influence the survival of the transplanted cells. Our results indicate that transplanted cell sheets may provide sufficient blood supply, not from the host myocardium but from the omentum tissue. Thus, we consider that the omentum flap technique could provide a well-organized vascular network, regardless of conditions of the host myocardium, to enhance the survival of the transplanted cells. Further studies are needed to explore the mechanisms underlying integration of the transplanted cells sheets into the heart and to develop methods to enhance the survival and functionality of the transplanted cells.

Cardiac tissue engineering is another strategy that uses stem cells for the treatment of heart failure. One of the major challenges of in vitro engineering techniques is to overcome the limited thickness of the construct because the maximum oxygen diffusion is limited to ≈200 μm^2. A few recent methodologies have successfully yielded thicker engineered cardiac tissues. Cardiomyocytes in the Matrigel matrix were implanted with an arteriovenous blood vessel loop in vivo, and spontaneously contracting, thick, 3-dimensional constructs with extensive vascularization were thus attained.[32] The cell-sheet method, which is a scaffold-free system, is also an in vitro engineering technique. A cell sheet, itself, has a potential to induce angiogenesis quickly after implantation, and cell-dense 1-mm thick cardiac tissue was developed by repeated transplantation of triple-layered rat neonatal cardiac cell sheets.[33] This cardiac graft generated by this method, however, would be limited in use as a graft transplanted to the heart because of the lack of responsible large arteries and veins that can be revascularized after transplantation to the heart. In the present study, we used the omentum as a blood supply source after cell transplantation and demonstrated that the omentum enhanced angiogenesis and survival of the delivered cells. In addition, the omentum can easily be handled and mobilized, preserving its vascular network. The omentum, therefore, is a promising tool for in vivo vascularization in cardiac tissue engineering, although further studies with technological development would be needed for this strategy.

In conclusion, covering of the omentum flap over the transplanted hiPS-CM cell sheets on the myocardium effectively promoted angiogenesis, leading to enhanced survival of the hiPS-CMs. These results warrant further investigations as a clinically relevant strategy to enhance hiPS-CM transplantation therapy for heart failure.

Acknowledgments

We thank Shigeru Matsumi, Yuka Fujiwara, Hiromi Nishinaka, and Akima Harada for their excellent technical assistance.

Sources of Funding

This work was supported by the Japan Society for the Promotion of Science Core-to-Core Program and the Highway Program for the Realization of Regenerative Medicine of the Japanese Ministry of Education Sports, Science, and Technology.

Disclosures

Dr Shimizu is a consultant for CellSeed, Inc. Dr Okano is an Advisory Board Member in CellSeed, Inc, and an inventor/developer designated on the patent for temperature -responsive culture surfaces. The other authors report no conflicts.

References

1. Menasche P. Cardiac cell therapy: lessons from clinical trials. *J Mol Cell Cardiol*. 2011;50:258–265.
2. Hsiao LC, Carr C, Chang KC, Lin SZ, Clarke K. Stem cell-based therapy for ischemic heart disease. *Cell Transplant*. 2013;22:663–675.
3. Chimenti I, Smith RR, Li TS, Gerstenblith G, Messina E, Giacomello A, Marbán E. Relative roles of direct regeneration versus paracrine effects of human cardiosphere-derived cells transplanted into infarcted mice. *Circ Res*. 2010;106:971–980.
4. Tang XL, Rokosh G, Sanganalmath SK, Yuan F, Sato H, Mu J, Dai S, Li C, Chen N, Peng Y, Dawn B, Hunt G, Leri A, Kajstura J, Tiwari S, Shirk G, Anversa P, Bolli R. Intracoronary administration of cardiac progenitor cells alleviates left ventricular dysfunction in rats with a 30-day-old infarction. *Circulation*. 2010;121:293–305.
5. Takahashi K, Tanabe K, Ohnuki M, Narita M, Ichisaka T, Tomoda K, Yamanaka S. Induction of pluripotent stem cells from adult human fibroblasts by defined factors. *Cell*. 2007;131:861–872.
6. Yu J, Vodyanik MA, Smuga-Otto K, Antosiewicz-Bourget J, Frane JL, Tian S, Nie J, Jonsdottir GA, Ruotti V, Stewart R, Slukvin II, Thomson JA. Induced pluripotent stem cell lines derived from human somatic cells. *Science*. 2007;318:1917–1920.
7. Yoshida Y, Yamanaka S. iPS cells: a source of cardiac regeneration. *J Mol Cell Cardiol*. 2011;50:327–332.
8. Shimizu T, Yamato M, Isoi Y, Akutsu T, Setomaru T, Abe K, Kikuchi A, Umezu M, Okano T. Fabrication of pulsatile cardiac tissue grafts using a novel 3-dimensional cell sheet manipulation technique and temperature-responsive cell culture surfaces. *Circ Res*. 2002;90:e40.
9. Zvibel I, Smets F, Soriano H. Anoikis: roadblock to cell transplantation? *Cell Transplant*. 2002;11:621–630.
10. Memon IA, Sawa Y, Fukushima N, Matsumiya G, Miyagawa S, Taketani S, Sakakida SK, Kondoh H, Aleshin AN, Shimizu T, Okano T, Matsuda H. Repair of impaired myocardium by means of implantation of engineered autologous myoblast sheets. *J Thorac Cardiovasc Surg*. 2005;130:1333–1341.
11. Sekine H, Shimizu T, Dobashi I, Matsuura K, Hagiwara N, Takahashi M, Kobayashi E, Yamato M, Okano T. Cardiac cell sheet transplantation improves damaged heart function via superior cell survival in comparison with dissociated cell injection. *Tissue Eng Part A*. 2011;17:2973–2980.
12. Sawa Y, Miyagawa S, Sakaguchi T, Fujita T, Matsuyama A, Saito A, Shimizu T, Okano T. Tissue engineered myoblast sheets improved cardiac function sufficiently to discontinue LVAS in a patient with DCM: report of a case. *Surg Today*. 2012;42:181–184.
13. Kawamura M, Miyagawa S, Miki K, Saito A, Fukushima S, Higuchi T, Kawamura T, Kuratani T, Daimon T, Shimizu T, Okano T, Sawa Y. Sheets in a porcine ischemic cardiomyopathy model. *Circulation*. 2012;126:S29–S37.
14. O'Shaugnessy L. Surgical treatment of cardiac ischemia. *Lancet*. 1937;232:185–94.
15. Bigelow WG, Basian H, Trusler GA. Internal mammary artery implantation for coronary heart disease. A clinical follow-up study on to eight years after operation. *J Thorac Cardiovasc Surg*. 1963;45:67–79.
16. Aldridge HE, Macgregor DC, Lansdown EL, Bigelow WG. Internal mammary artery implantation for the relief of angina pectoris: a follow-up study of 77 patients for up to 13 years. *Can Med Assoc J*. 1968;98:194–198.
17. Shrager JB, Wain JC, Wright CD, Donahue DM, Vlahakes GJ, Moncure AC, Grillo HC, Mathisen DJ. Omentum is highly effective in the management of complex cardiothoracic surgical problems. *J Thorac Cardiovasc Surg*. 2003;125:526–532.
18. Takaba K, Jiang C, Nemoto S, Saji Y, Ikeda T, Urayama S, Azuma T, Hokugo A, Tsutsumi S, Tabata Y, Komeda M. A combination of omental flap and growth factor therapy induces arteriogenesis and increases myocardial perfusion in chronic myocardial ischemia: evolving concept of biologic coronary artery bypass grafting. *J Thorac Cardiovasc Surg*. 2006;132:891–899.
19. Shudo Y, Miyagawa S, Fukushima S, Saito A, Shimizu T, Okano T, Sawa Y. Novel regenerative therapy using cell-sheet covered with omentum flap delivers a huge number of cells in a porcine myocardial infarction model. *J Thorac Cardiovasc Surg*. 2011;142:1188–1196.
20. Toyoda K, Tooyama I, Kato M, Sato H, Morikawa S, Hisa Y, Inubushi T. Effective magnetic labeling of transplanted cells with HVJ-E for magnetic resonance imaging. *Neuroreport*. 2004;15:589–593.
21. Miyoshi S, Flexman JA, Cross DJ, Maravilla KR, Kim Y, Anzai Y, Oshima J, Minoshima S. Transfection of neuroprogenitor cells with iron nanoparticles for magnetic resonance imaging tracking: cell viability, differentiation, and intracellular localization. *Mol Imaging Biol*. 2005;7:286–295.
22. Kraitchman DL, Heldman AW, Atalar E, Amado LC, Martin BJ, Pittenger MF, Hare JM, Bulte JW. *In vivo* magnetic resonance imaging of mesenchymal stem cells in myocardial infarction. *Circulation*. 2003;107:2290–2293.
23. Takehara N, Tsutsumi Y, Tateishi K, Ogata T, Tanaka H, Ueyama T, Takahashi T, Takamatsu T, Fukushima M, Komeda M, Yamagishi M, Yaku H, Tabata Y, Matsubara H, Oh H. Controlled delivery of basic fibroblast growth factor promotes human cardiosphere-derived cell engraftment to enhance cardiac repair for chronic myocardial infarction. *J Am Coll Cardiol*. 2008;52:1858–1865.
24. Mangi AA, Noiseux N, Kong D, He H, Rezvani M, Ingwall JS, Dzau VJ. Mesenchymal stem cells modified with Akt prevent remodeling and restore performance of infarcted hearts. *Nat Med*. 2003;9:1195–1201.
25. Li W, Ma N, Ong LL, Nesselmann C, Klopsch C, Ladilov Y, Furlani D, Piechaczek C, Moebius JM, Lützow K, Lendlein A, Stamm C, Li RK, Steinhoff G. Bcl-2 engineered MSCs inhibited apoptosis and improved heart function. *Stem Cells*. 2007;25:2118–2127.
26. Tulloch NL, Muskheli V, Razumova MV, Korte FS, Regnier M, Hauch KD, Pabon L, Reinecke H, Murry CE. Growth of engineered human myocardium with mechanical loading and vascular coculture. *Circ Res*. 2011;109:47–59.
27. Matsuura K, Wada M, Shimizu T, Haraguchi Y, Sato F, Sugiyama K, Konishi K, Shiba Y, Ichikawa H, Tachibana A, Ikeda U, Yamato M, Hagiwara N, Okano T. Creation of human cardiac cell sheets using pluripotent stem cells. *Biochem Biophys Res Commun*. 2012;425:321–327.
28. Yu T, Miyagawa S, Miki K, Saito A, Fukushima S, Higuchi T, Kawamura M, Kawamura T, Ito E, Kawaguchi N, Sawa Y, Matsuura N. *In vivo* differentiation of induced pluripotent stem cell-derived cardiomyocytes. *Circ J*. 2013;77:1297–1306.
29. Uccelli A, Moretta L, Pistoia V. Mesenchymal stem cells in health and disease. *Nat Rev Immunol*. 2008;8:726–736.
30. Chandra A, Srivastava RK, Kashyap MP, Kumar R, Srivastava RN, Pant AB. The anti-inflammatory and antibacterial basis of human omental defense: selective expression of cytokines and antimicrobial peptides. *PLoS One*. 2011;6:e20446.
31. Pearl JI, Lee AS, Leveson-Gower DB, Sun N, Ghosh Z, Lan F, Ransohoff J, Negrin RS, Davis MM, Wu JC. Short-term immunosuppression promotes engraftment of embryonic and induced pluripotent stem cells. *Cell Stem Cell*. 2011;8:309–317.
32. Morritt AN, Bortolotto SK, Dilley RJ, Han X, Kompa AR, McCombe D, Wright CE, Itescu S, Angus JA, Morrison WA. Cardiac tissue engineering in an *in vivo* vascularized chamber. *Circulation*. 2007;115:353–360.
33. Shimizu T, Sekine H, Yang J, Isoi Y, Yamato M, Kikuchi A, Kobayashi E, Okano T. Polysurgery of cell sheet grafts overcomes diffusion limits to produce thick, vascularized myocardial tissues. *FASEB J*. 2006;20:708–710.

Cell Transplantation, Vol. 23, pp. 167–179, 2014
Printed in the USA.

0963-6897/14 $90.00 + .00
DOI: http://dx.doi.org/10.3727/096368912X658007
E-ISSN 1555-3892
www.cognizantcommunication.com

Autologous G-CSF-Mobilized Peripheral Blood CD34$^+$ Cell Therapy for Diabetic Patients With Chronic Nonhealing Ulcer

Rica Tanaka,*† Haruchika Masuda,† Shunichi Kato,† Kotaro Imagawa,‡ Kazuo Kanabuchi,§ Chie Nakashioya,¶ Fumiaki Yoshiba,¶ Tsuyoshi Fukui,‡ Rie Ito,† Michiru Kobori,† Mika Wada,† Takayuki Asahara,† and Muneo Miyasaka‡

*Department of Plastic and Reconstructive Surgery, Juntendo University School of Medicine, Tokyo, Japan
†Department of Regenerative Medicine, Tokai University School of Medicine, Isehara, Kanagawa, Japan
‡Department of Plastic and Reconstructive Surgery, Tokai University School of Medicine, Isehara, Kanagawa, Japan
§Department of Cardiovascular Surgery, Tokai University School of Medicine, Isehara, Kanagawa, Japan
¶Department of Blood Transfusion Service, Cell Transplantation and Regenerative Medicine, Tokai University School of Medicine, Isehara, Kanagawa, Japan

Recently, animal studies have demonstrated the efficacy of endothelial progenitor cell (EPC) therapy for diabetic wound healing. Based on these preclinical studies, we performed a prospective clinical trial phase I/IIa study of autologous G-CSF-mobilized peripheral blood (PB) CD34$^+$ cell transplantation for nonhealing diabetic foot patients. Diabetic patients with nonhealing foot ulcers were treated with 2×10^7 cells of G-CSF-mobilized PB CD34$^+$ cells as EPC-enriched population. Safety and efficacy (wound closure and vascular perfusion) were evaluated 12 weeks posttherapy and further followed for complete wound closure and recurrence. A total of five patients were enrolled. Although minor amputation and recurrence were seen in three out of five patients, no death, other serious adverse events, or major amputation was seen following transplantation. Complete wound closure was observed at an average of 18 weeks with increased vascular perfusion in all patients. The outcomes of this prospective clinical study indicate the safety and feasibility of CD34$^+$ cell therapy in patients with diabetic nonhealing wounds.

Key words: Nonhealing diabetic wound; Endothelial progenitor cells (EPC); Autologous cell therapy; Vasculogenesis; Wound healing

INTRODUCTION

Diabetic patients with nonhealing chronic ulcer are increasing yearly. Most nonhealing diabetic ulcers with peripheral vascular disease are difficult to cure, and once all conventional treatment modalities are exhausted, amputation is the final solution. More than 40–60% of nontraumatic lower extremity amputations are related to diabetic foot. It is also reported that individuals with diabetes have 15 to 46 times greater risk of high-level lower extremity amputations than those without diabetes (29). In addition, 5-year mortality rates after lower extremity amputation for diabetics, critical limb ischemia, and peripheral artery disease range from 39% to 68% (15). Furthermore, the economic burden of diabetic foot ulcer is estimated to be $98 billion per year (26). These data suggest the importance and necessity of alternative and more effective treatment option for diabetic patients with nonhealing ulcers.

After the discovery of endothelial progenitor cells (EPCs) in 1997, these vascular stem cells became the subject of intense experimental and clinical investigation for angiogenesis and wound healing. EPCs are an immature cell population that possesses an enhanced potential to differentiate into mature endothelial cells (2). EPCs can be isolated as cluster of differentiation 34-positive cells (CD34$^+$) and CD133$^+$ mononuclear cells (MNCs) from adult bone marrow (BM) and peripheral blood (2,9). EPCs mainly reside in the bone marrow and are mobilized into the peripheral blood with tissue ischemia or systematic administration of granulocyte colony-stimulating factor (G-CSF), vascular endothelial growth factor (VEGF), or estrogen (22,31). Mobilized EPCs will be home to ischemic sites for vascular repair. Preliminary studies support the potential of EPC therapy for angiogenesis and wound healing, and systemic (27) and local transplantation of EPCs (30) has become an alternative

Received March 22, 2012; final acceptance October 9, 2012. Online prepub date: October 25, 2012.
Address correspondence to Rica Tanaka, M.D., Ph.D., Department of Plastic and Reconstructive Surgery, Juntendo University School of Medicine, 2-1-1 Hongo Bunkyo-ku, Tokyo, 113-8421, Japan. Tel: +81-03-8313-3111; E-mail: rtanaka@juntendo.ac.jp

therapeutic option for diabetic ulcers. In murine diabetic ulcer, human EPCs are incorporated into the wound bed of diabetic mice following local injection and participate in neovascularization with recipient's endothelial cells, resulting in enhancement of wound vascular density and higher wound closure rate (28). Lin et al. also demonstrated that topical application of bone marrow-derived progenitor cells accelerates diabetic wound healing and increases wound vasculogenesis (19). These promising results encouraged clinical application of EPC transplantation for improvement of nonhealing diabetic ulcer. Until now, several researchers have investigated and reported the efficacy of autologous bone marrow and peripheral blood MNCs on patients with diabetic ulcers; however, the efficacy of purified EPC transplantation is not yet investigated (13,18).

Here we report a phase I/IIa clinical trial of transplantation of autologous and G-CSF-mobilized $CD34^+$ cells in patients with intractable diabetic ulcer. G-CSF was used to efficiently mobilize bone marrow-derived EPCs to peripheral blood, and the mobilized $CD34^+$ cells were isolated as the EPC-enriched fraction.

MATERIALS AND METHODS

Ethical Conduct of Research

The authors have obtained appropriate institutional review board approval or have followed the principles outlined in the Declaration of Helsinki for all human experimental investigation. In addition, appropriate informed consent has been obtained from all patients by the investigator in charge.

Study Design

This phase I/IIa study was conducted from July 2005 to March 2010 at Tokai University School of Medicine Department of Plastic and Reconstructive Surgery. The protocol was reviewed and approved by the Ethics Committee of the Tokai University School of Medicine, Kanagawa, Japan. The primary end point of this trial is safety, and the secondary end point is primary efficacy. Patients providing informed consent had type 2 diabetes with a nonhealing chronic ulcer. If wounds were on both feet, the foot with a more severe wound was treated with autologous G-CSF-mobilized peripheral blood $CD34^+$ cells. Inclusion criteria included (1) type 2 diabetic patients of ages 20 to 70 years with a nonhealing chronic wound deeper than the subcutaneous layer of the skin. The wound was determined as nonhealing and chronic when the wound was treated with current standard care for diabetic foot ulcer by a wound care specialist for at least 3 months prior to the therapy with less than 40% of wound closure. There were no limitations of the wound size. (2) Patients with strict diabetic control of glycated hemoglobin (HbA1c) below 6.5%. The exclusion criteria included (1) collagen tissue disease or malignant disease, (2) an ejection fraction lower than 50%, (3) interventional treatment required for coronary or cerebral artery stenosis within 6 months, (4) diabetic retinal bleeding, (5) hematological disorder, (6) onset of myocardial infarction or cerebral infarction within the last 6 months, (7) side effects arising from G-CSF pharmaceutical or apheresis procedures, and (8) wound infection. Written informed consent for participation was obtained from all subjects. All patients did not receive any medication changes pre- and post-EPC injection therapy. Since the study was a phase I/IIa clinical trial, controls for the study were not established.

Study Procedures

Screening assessments within 14 days before treatment included medical history, review of inclusion and exclusion criteria, review of medications, vital signs, physical examination, chest X-ray (Shimadzu, Kyoto, Japan), urinalysis, blood collections for hematology [complete blood count (CBC) and differential], clinical chemistry [bilirubin, alkaline phosphatase, alanine aminotransferase (ALT), aspartate aminotransferase (AST), lactate dehydrogenase (LDH), urea nitrogen, creatinine, glucose, uric acid, calcium, phosphorus, total protein, albumin, electrolytes, amylase, cholesterol, triglycerides], and HbA1c. All blood-related measurements were performed by the blood testing central laboratory at the Hospital of Tokai University, Kanagawa, Japan. Patients underwent cardiac echography, abdominal echography (Toshiba, Tokyo, Japan), and cerebral, chest, and abdominal computed tomography (CT; Siemens, Tokyo, Japan) to rule out any conditions listed in the exclusion criteria. During the 3-month screening period, patients continued to receive the standard care for diabetic feet. Foot ulcers were photographed using a digital camera with a 1-cm^2 size sticker marked near the wound. The area of the ulcer was calculated by measuring the size of the photographed ulcer divided by the photographed 1-cm^2 size marker using VH analyzer (Keyence Corp, Osaka, Japan). Vascular perfusion was evaluated by using the following parameters: ankle brachial pressure index (ABI), skin perfusion pressure (SPP), and transcutaneous oxygen pressure (TcO_2). Angiographic analysis was performed for cases with severe peripheral vascular disease. TcO_2 was measured with an oxymonitor (PO-850, Sumitomo-Hightechs, Tokyo, Japan). The probe was placed at the dorsum pedis, and the skin was heated to 42°C (4). SPP was measured with the PAD3000 (Vasamedics, St. Paul, MN, USA) proximal to the wound with an exclusive cuff (5,6). These physiological examinations were performed while the patient was in a supine position after more than 30 min of rest in a temperature-controlled room. Angiographic examinations were performed with the intra-arterial digital subtraction angiography (IA-DSA) technique. The

standard Seldinger approach was used as follows: the top of the 4 Fr catheters was placed at the external iliac artery, and iohexol (Omnipaque, 300 mg of iodine/ml; Daiichi Pharmaceutical, Tokyo, Japan) was injected automatically using an infusion pump at a speed of 20 ml/s for 2 s. Wound care was standardized throughout the entire study by using several different dressing types dependent on the type of the wound (e.g., dry, wet, and intermediate) with daily dressing changes and use of an offloading device by a wound care specialist. Minor debridement of necrotic tissue without general anesthesia was performed as regular wound care. Major debridement was performed only at the time of cell transplantation under general anesthesia.

Treatment Period

Collection of Peripheral Blood CD34+ Cells. Patients who met the criteria were admitted to the hospital, and 10 μg/kg/day of G-CSF (Filgrastim; Gran®, Kyowa Hakko Kirin, Co. Ltd., Tokyo, Japan) was injected subcutaneously for 5 days. Blood counts, peripheral leukocyte differential counts, and peripheral CD34+ cell counts were determined daily. If leukocyte count exceeded 50,000/μl, the dose of G-CSF was reduced to one half. On day 5, peripheral blood MNC collection was performed with the COBE SPECTRA apheresis system (Gambro BCT, Lakewood, CO, USA). MNC collection was followed by purification of CD34+ cells by means of a magnetic-activated cell sorting system (CliniMACS, Milteny Biotech, Bergisch Gladbach, Germany).

Administration of Isolated CD34+ Cells. Debridement and transplantation of CD34+ cells were performed under general anesthesia on the same day of cell isolation. After debridement and irrigation of the wound, CD34+ cells were injected intramuscularly within 20 cm surrounding the wound with a 26-gauge needle (Nipro Corporation, Osaka, Japan). A total of 2×10^7 CD34+ cells/patient was administered by 20 injections, each injection containing 1×10^6 cells/0.25 ml saline (0.25 ml×20 sites, 1.5–2.0 cm deep). Saline gauze dressing was placed over the treated wound immediately after the treatment to avoid cell damage, and standard of wound care was continued starting postoperative day 1. The patient was discharged from the hospital the following day unless any side effects due to the CD34+ cell therapy were seen. Current standard of care for diabetic foot was performed starting on the day of discharge.

End Points

The primary end point of this study is to evaluate the safety, and the secondary end point is to evaluate efficacy 12 weeks posttherapy. No gold standard efficacy end points have been established for small size, early phase clinical trials in patients with diabetic foot, so we originally prespecified the efficacy score as a surrogate end point so that we could simultaneously evaluate subjective and objective parameters in the study. Twelve weeks posttherapy was determined as the time point of evaluation in reference to other clinical trial reports assessing diabetic wound healing because all patients included in the study had nonhealing wound for more than 3 months (20,37). The adverse effects were evaluated according to the National Cancer Institute Common Terminology Criteria for Adverse Events (NCI CTCAE version 3 http://ctep.cancer.gov/protocolDevelopment/electronic_applications/docs/ctcaev3.pdf). Full physical examination, blood collection for hematology, clinical chemistry, chest X-ray, abdominal echo, cardiac echo, cerebral CT, chest CT, and abdominal CT were performed to find if any conditional change existed after the therapy. C-Reactive protein was measured by latex-enhanced immunoturbidimetric assay (Eiken Chemical Co. Ltd., Tokyo, Japan). The efficacy score was defined as the sum of four scores, each of which measured a difference in the parameters between baseline and 12 weeks after cell therapy: (1) percent wound closure calculated by VH analyzer as previously mentioned in the study procedure section (wound needing minor or major amputation was evaluated and performed at 12 weeks posttherapy; major amputation is an amputation of below the knee or above the knee or a procedure proximal to this level, whereas minor

Table 1. Efficacy Score

Parameter	Score Value
Wound closure at post-12 weeks score according to Δ from baseline	
76–100% wound closure	2
36–75% wound closure	1
0–35% wound closure	0
Minor amputation	−1
Major amputation	−2
SPP score 12 weeks after treatment	
>40 mmHg	2
30–40 mmHg	1
<30 mmHg	0
No change	−1
Worsening	−2
Wong-Baker FACES Pain Rating Scale score	
Improvement by ≥2 steps	2
Improvement by 1 step	1
No change	0
Worsening by 1 step	−1
Worsening by ≥2 steps	−2
Recurrence	
No recurrence more than a year	2
No recurrence within a year	1
Recurrence but healed	0
Recurrence but nonhealing	−1
Recurrence with amputation	−2

The efficacy score = (wound closure + SPP + Wong-Baker FACES Pain Scale) post-12 weeks therapy + Recurrence. Range: −2 to 2 for each category. SPP, skin perfusion pressure.

Table 2. Exposure and Outcome for All Patients Treated With Autologous G-CSF-Mobilized Peripheral Blood CD34$^+$ Cell Therapy

Case	Age/ Sex	PMH	Location of Ulcer	Nonhealing Time Pretherapy (Weeks)	Ulcer Size at Baseline (cm)	HbA1C	Time of Complete Wound Closure (Weeks)	Amputation	SPP	ADL Posttherapy	Time Posttherapy	Ulcer Recurrence	Adverse Effects
1	41/M	DM CRF on HD PAD	Rt 1st, 2nd, 3rd toe	22	4.4×3.6	5.6	12	None	↑	Ambulant	4.8	None	None
2	70/F	DM CRF on HD PAD	Rt foot	74	2×1.5	5.4	12	None	↑	Ambulant	4	Within 1 year/ nonhealing	None
3	63/M	DM CRF on HD PAD CVD	Lt. 5th toe	100	2.7×1.5	4.7	18	Minor	↑	Ambulant	3	Within 1 year/ healed	None
4	53/M	DM CRF on HD PAD	Rt. 1st toe	33	3×2	4.9	26	Minor	↑	Ambulant	2	Within 1 year/ healed	None related/ restenosis of Pop. A
5	63/M	DM CRF on HD PAD	Lt foot	26	4.5×6.0	5.8	16	None	↑	Ambulant	2	None	None

G-CSF, granulocyte colony-stimulating factor; CD34, cluster of differentiation 34; PMH, past medical history; HbA1c, glycated hemoglobin; SPP, skin perfusion pressure; ADL, activities of daily living; DM, diabetes mellitus; CRF, chronic renal failure; HD, hemodialysis; PAD, peripheral artery disease; Pop. A, popliteal artery.

Table 3. Outcome of Mobilization, Harvest, and Isolation of CD34+ Cells

Case	% CD34+ Cells in PB by Flow Cytometry	Total MNCs After Apheresis	Total CD34+ Cells After Apheresis	Total Isolated CD34+ Cells	Total Isolated CD34+ Cells/kg	Purity of CD34+ Cells
1	0.31%	4.02E+10	1.19E+08	7.21E+07	9.01E+05	80%
2	0.08%	1.16E+10	1.23E+07	6.14E+06	1.23E+05	50%
3	0.40%	2.31E+10	8.59E+07	4.60E+07	7.67E+05	83%
4	0.33%	2.59E+10	8.86E+07	4.28E+07	5.35E+05	82%
5	0.28%	3.34E+10	9.23E+07	4.04E+07	5.05E+05	56%
Average	0.28%	2.68E+10	7.96E+07	4.15E+07	5.66E+05	70%
SD	0.12%	1.08E+10	3.99E+07	2.35E+07	3.29E+05	15.82%

The frequency of CD34+ cells in the peripheral blood at day 5 post-G-CSF injection was $0.28 \pm 0.1\%$ by flow cytometry. The average apheresis product number was $2.68 \pm 1 \times 10^{10}$, and the average of total CD34+ cells obtained after magnetic sorting was $7.96 \pm 4.0 \times 10^{7}$. Flow cytometry revealed that the purity and viability of the CD34+ cell fraction following magnetic sorting were $70 \pm 15.8\%$. PB, peripheral blood; MNCs, mononuclear cells.

amputation is classified as all other partial foot or toe resection) (10); (2) skin perfusion pressure (SPP) in the treated foot; (3) Wong–Baker FACES Pain Rating Scale score (http://www.wongbakerfaces.org/), evaluation of pain in the treated leg; and (4) recurrence of the treated wound. Each score is given a range of plus 2 to minus 2 points; the best response is assigned plus 2, and the worst outcome is assigned minus 2. The efficacy score sum is in the range of +8 to −8 (Table 1). The patients visited the clinic 2 weeks, 4 weeks, 8 weeks, and 12 weeks postoperatively to evaluate safety and efficacy. The patients were still followed every 4 weeks when complete wound closure was not seen at 12 weeks posttherapy. The photographs were taken for percent wound closure, and ABI, SPP, and TcO_2 were tested for vascular perfusion at each visit. Angiographic analysis was performed for cases with severe peripheral vascular disease 12 weeks postoperatively. Each patient evaluated pain level at baseline and at 12 weeks after transplantation using the Wong–Baker FACES Pain Rating Scale (7). A clinical research coordinator interviewed each patient regarding the level of psychroesthesia, paresthesia, and the required quantity of analgesic drugs at baseline and at 12 weeks after transplantation. Recurrence of the wound was evaluated every 4 weeks posttherapy at each clinical visit. The recurred wounds were treated by standard of wound care and evaluated for time of wound closure. The efficacy score was validated by two individual physicians not included in the study.

Quality Analysis of CD34+ Cells

CD34+ cells isolated for transplantation were labeled with fluorescein isothiocyanate (FITC)-conjugated anti-CD34 (BD Biosciences, San Jose, CA, USA) and phycoerythrin (PE)-conjugated anti-KDR [kinase insert domain receptor or vascular endothelial growth factor receptor 2 (VEGFR2); BD Biosciences] antibodies for 20-min incubation at 4°C. Cells were then analyzed

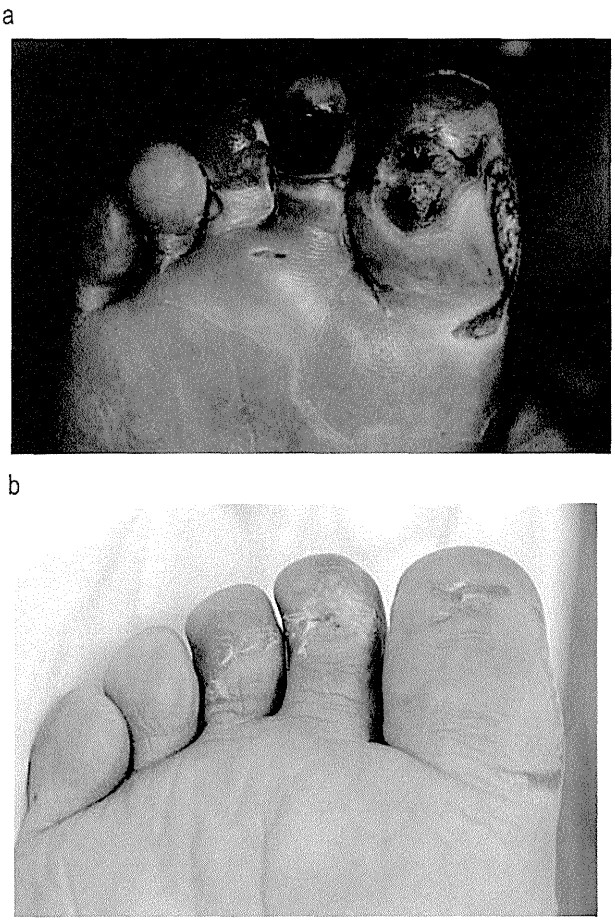

Figure 1. Case 1: A 41-year-old male who was diagnosed with diabetes at age 30 and currently undergoing dialysis. (a) Pretherapy: the ulcer seen in the picture was not healing for 22 weeks. (b) Three months posttherapy. After cluster of differentiation 34-positive (CD34+) cell therapy, the wound healed rapidly, and wound closure had occurred by 12 weeks after the therapy. No recurrence was seen for 4.8 years posttherapy. Skin perfusion pressure (SPP) measured proximal to the wound showed 13 mmHg pretherapy and 75 mmHg 12 weeks posttransplant.

using FACSCalibur and CellQuest Pro software (Becton Dickinson, Franklin Lakes, NJ, USA).

EPC Colony-Forming Assay

The vasculogenic potential of isolated peripheral blood $CD34^+$ cells was assessed using the EPC colony-forming assay (EPC-CFA) as previously described (17,21,32). Briefly, isolated 3,000 $CD34^+$ cells were suspended in 300 µl of 30% fetal bovine serum (FBS; Nichirei Bioscience Inc., Tokyo, Japan)/Iscove's modified Dulbecco's media (IMDM; Gibco) and mixed with 3 ml of previously stored EPC-CFA working medium (Methocult, Stem Cell Technologies, Vancouver, BC, Canada). A total of 1,000 $CD34^+$ cells/dish were seeded into a 35-mm hydrophilic tissue culture dish (BD Falcon, Bedford, MA, USA; 1 ml working medium to one dish, a total of three dishes per sample). After 18 days, the number of total EPC colony-forming units (EPC-CFU) was counted by two investigators who were blinded to the experimental conditions.

Statistical Analysis

All data are presented as the mean ± standard deviation. Student's *t* test was performed to assess statistical significance between the two groups.

A Kruskal–Wallis one-way ANOVA with Tukey–Kramer post hoc analysis was performed when comparisons involved more than two groups. Significance was considered to be $p < 0.05$. The statistical program used for the analysis of all data was Graph Pad Prism 5 (Graph pad Software, Inc., La Jolla, CA, USA).

RESULTS

Patient Characteristics

A total of five patients were enrolled in the trial. The characteristics of all patients enrolled in the trial are listed in Table 2. The age ranged from 41 to 70 years old. All patients had diabetes and chronic renal failure with hemodialysis as past medical history. Blood sugar levels were controlled for all patients, and hbA1C was below 6.5%. All of the wounds extended into bone or tendon and were located in the digits of the foot. The average size of the wound was 3.3 ± 1.1 cm^2 $\times 2.92 \pm 1.9$ cm^2. The average wound history prior to EPC therapy was 34 ± 23 weeks (240 days). Average ABI was 0.9 ± 0.17. All patients had low skin perfusion pressure (SPP: 14.8 ± 5.3) proximal to the wound, indicating peripheral vascular disease. Cases 4 and 5 had percutaneous transluminal angioplasty (PTA) 3 months prior to the therapy.

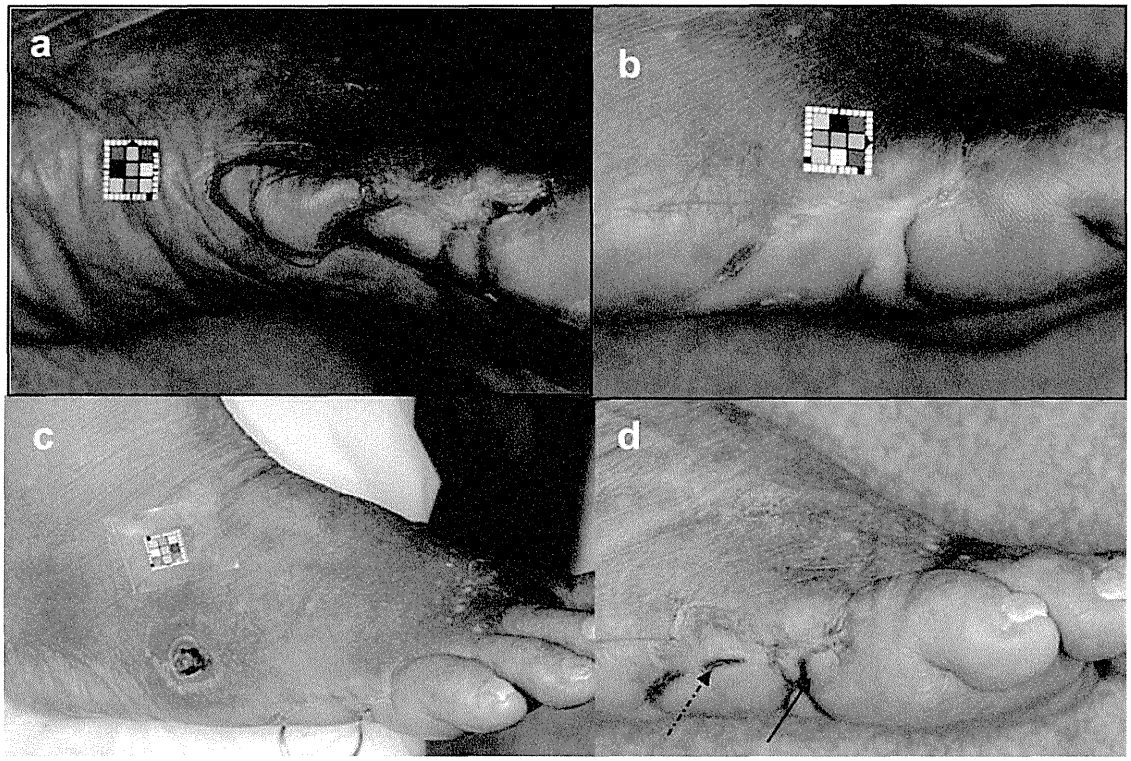

Figure 2. Case 2: A 70-year-old female with 48 years of diabetes and 28 years of chronic renal failure (CRF) on hemodialysis. (a) Pretherapy: the ulcer with a deep pocket reaching to the fifth metatarsal bone located in the lateral side of the right foot was nonhealing for 74 weeks. SPP was 10 mmHg pretherapy. (b) Posttherapy: the ulcer healed completely, and SPP increased to 45 mmHg after 12 weeks posttherapy. (c) One year posttherapy. (d) The dotted arrow shows cured heterotrophic ulcer 2 years posttherapy. The solid arrow shows ulcer recurrence.

Outcome of Mobilization, Harvest, and Isolation of CD34+ Cells

G-CSF was administered 10 μg/kg/day for 5 days for all patients. The frequency of $CD34^+$ cells in the peripheral blood at day 5 post-G-CSF injection was $0.3 \pm 0.1\%$ by flow cytometry analysis. The average apheresis product number was $2.7 \pm 1 \times 10^{10}$, and the average of total $CD34^+$ cells obtained after magnetic sorting by CliniMACS was $8.0 \pm 4.0 \times 10^7$. Flow cytometry revealed that the purity and viability of the $CD34^+$ cell fraction following magnetic sorting were $70 \pm 15.8\%$. The number of $CD34^+$ cells isolated was significantly low for Case 2 (1.23×10^5/kg) and high for Case 1 (9.0×10^5/kg) (Table 3).

Safety Evaluation

Neither death (NCI CTCAE grade 5) nor life-threatening adverse events (grade 4) were observed during the 12-week follow-up after cell therapy. In contrast, mild to moderate adverse events (grades 1–2) were observed as G-CSF-related events in all patients. Symptoms such as bone pain ($n=5$), headache ($n=1$), fever ($n=1$), and C-reactive protein (CRP) elevation ($n=1$) seen were transient and disappeared without permanent damage. There were no adverse events following general anesthesia. No episodes of site infection following cell injections were noted. There was no incidence of pathogenic angiogenesis after serial examination of fundus oculi.

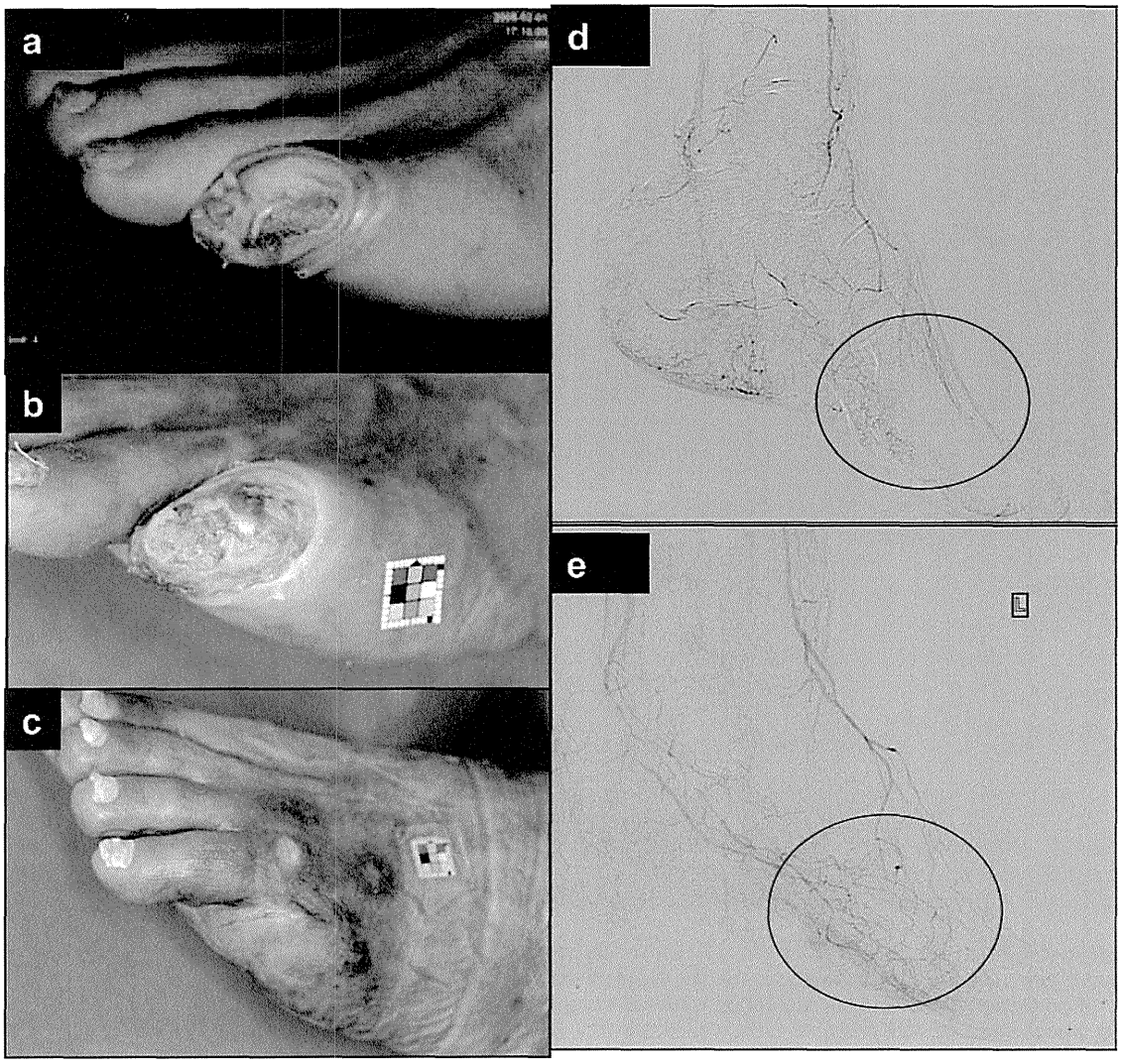

Figure 3. Case 3: A 63-year-old male with diabetes and CRF on hemodialysis. (a) The ulcer on the left fifth toe seen in the picture was nonhealing for 14 weeks. Dorsal SPP was 10 mmHg at this point. (b) The ulcer after 12 weeks posttherapy; the ulcer did not heal at this point, but SPP increased to 45 mmHg. (c) The patient underwent minor amputation of the fifth toe, and the wound completely healed 28 weeks after the therapy. (d) Angiography pretherapy; circled area is avascular. (e) Angiography 12 weeks posttherapy showed increased vascularity in the avascular area pretherapy.

Efficacy Evaluation

The efficacy score at 12 weeks was more than or equal to 2 in all patients, indicating the efficacy of transplantation of $CD34^+$ cells.

Wound Closure. Only two out of five patients (Case 1 and Case 2; Figs. 1 and 2) had complete wound closure within 12 weeks of evaluation. Since the remaining sequestrum was obstructing wound healing, two out of five patients (Case 3 and Case 4; Figs. 3 and 4) received further debridement resulting as minor amputation. In Case 5, the patient had the largest wound pretherapy, which had healed within 16 weeks posttherapy (Fig. 5). Although only two had complete wound closure by 12 weeks posttherapy and two resulted as minor amputation, all patients had complete wound closure without any major amputation at an average of 18.8 weeks (131.6 days) (Fig. 6). During the trial, Case 4 had sudden stenosis of popliteal artery after 8 weeks of therapy, which had healed after percutaneous transluminal angioplasty (PTA).

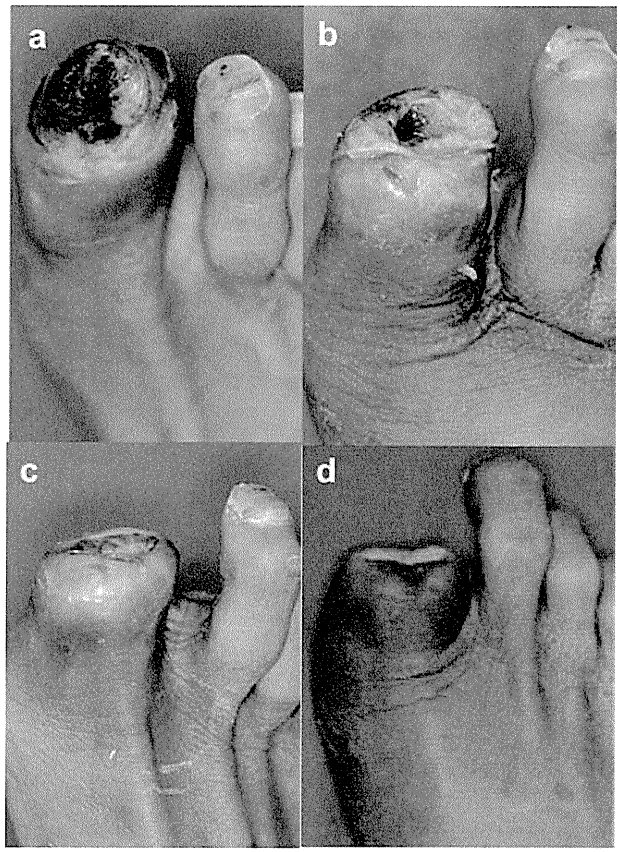

Figure 4. Case 4: A 53-year-old male with 15 years of diabetes and 9 years of CRF on hemodialysis. (a) The ulcer on the right toe pretherapy, which did not heal for 33 weeks. (b) Eight weeks after the therapy, SPP proximal to the wound, which was 14 mmHg, suddenly dropped to 2 mmHg. Angiogram showed stenosis of popliteal artery, and emergency percutaneous transluminal angioplasty (PTA) was performed. (c) At 12 weeks posttherapy. SPP increased to 58 mmHg with increased granulation. (d) At 26 weeks posttherapy. The wound completely healed at this point, and the patient was wound free for more than 2 years with an average SPP of 42 ± 11 mmHg.

Peripheral Vascular Perfusion. There was no significant change in resting ABI pretherapy and posttherapy (0.9 ± 0.2 vs. 0.9 ± 0.2), but SPP (14.5 ± 5.3 vs. 53.6 ± 16.3; $p < 0.01$) and TcO_2 (27.8 ± 8.2 vs. 56.0 ± 7.2; $p < 0.01$) proximal to the wound showed a significant increase 12 weeks after the therapy in all patients (Fig. 6). Angiography performed 12 weeks posttherapy showed increased vascularity in the deep plantar artery for Cases 3 and 5 (Figs. 3 and 5).

Pain Scale. Four out of five patients had limb and foot pain before the therapy, which began to be relieved 4 weeks after the therapy. The average pain level evaluated using the Wong–Baker FACES Pain Rating Scale of 3.2 ± 2.1 at baseline decreased to 0.6 ± 0.9 at 3 months after therapy ($p < 0.05$) (Fig. 6).

Recurrence. The ulcer of Cases 1 and 5 had not yet recurred after more than 2 years of cell therapy. Cases 3 and 4 showed recurrence of the ulcer within 1 year after the therapy, but it was rapidly cured in a few weeks (3 weeks for Case 3 and 2 weeks for Case 4) after standard care. However, the recurred ulcer for Case 2 did not heal even after 3 years of standard care (Fig. 2).

Vasculogenic Potential of Transplanted $CD34^+$ Cells

Case 1 with wound closure at 12 weeks posttherapy and no incidence of heterotopic ulcers or recurrence demonstrated a significantly higher number of total EPC-CFU compared to the other four cases (Case 1: 25 ± 6 vs. Case 2: 4 ± 2, Case 3: 11 ± 1, Case 4: 11 ± 1.5, Case 5: 16 ± 1; $p < 0.01$) (Fig. 7). Flow cytometry of CD34 and KDR double-positive cell percentages within the transplanted $CD34^+$ cells showed similar results to EPC-CFU. Case 1 showed a significantly higher number of CD34/KDR double-positive cell percentage compared to the other four cases (2.8 vs. 0.5, 0.37, 1.49, 1.67), suggesting that transplanted $CD34^+$ cells with higher vasculogenic potential exhibit accelerated wound healing and better prognosis (Fig. 7).

DISCUSSION

To the best of our knowledge, the present study is the first clinical trial of transplantation of autologous and purified $CD34^+$ cells into diabetic patients on hemodialysis who were suffering from nonhealing chronic wounds for more than 3 months. Previous studies on autologous transplantation of bone marrow or peripheral blood stem cells for diabetic ulcers were focused on administrating mononuclear cells to more acute or subacute wounds as cell population including EPCs (13). Since application of peripheral blood or bone marrow mononuclear cells